



Cite this: *Polym. Chem.*, 2024, **15**, 1975

Ring-opening (co)polymerization of chiral seven-membered lactones mediated by achiral yttrium catalysts: insights into the catalyst stereocontrol by mass spectrometry†

Ali Dhaini,^a Jérôme Ollivier,^a Nicolas Le Yondre,^b Ali Alaeddine,^c Sophie M. Guillaume  ^{*a} and Jean-François Carpentier  ^{*a}

Ring-opening polymerization (ROP) of cyclic esters is a preferred approach for the preparation of various polyesters with controlled microstructures. In this work, the ROP of chiral seven-membered substituted- ϵ -caprolactones, namely 1-methyl- ϵ -caprolactone (CL^{Me}) and 1-*n*-butyl- ϵ -caprolactone (CL^{nBu} , aka ϵ -decalactone), was investigated to assess the potential stereoregularity of the resulting poly(lactones). The reactions mediated by yttrium complexes $Y\{ON(N)O^{R2}\}$ based on non-chiral diamino-*bis(o,p-di-substituted-phenolate)* ligands, associated with an exogeneous alcohol as a co-initiator, were effectively catalyzed – that is, with good control over molar mass values, narrow dispersity, and chain-end fidelity. However, the tacticity of the homopolymers obtained from racemic monomers *rac*- CL^{Me} or *rac*- CL^{nBu} could not be evidenced by NMR spectroscopy, as outlined in previous literature reports. Alternatively, the ring-opening copolymerization (ROCOP) of equimolar mixtures of (*R*)- CL^{nBu} /*(S*)- CL^{Me} enabled, indirectly, the assessment of the catalyst stereocontrol through the evaluation of the ultimate degree of alternation of the inserted units of each comonomer. While NMR spectroscopy again did not enable unambiguous evaluation of the copolymer topology/sequence, detailed MALDI-ToF and high-resolution ESI mass spectrometric analyses rewardingly revealed two major series of macromolecules, cyclic and linear ones. Both series of macromolecules showed randomly distributed units of both comonomers, thereby evidencing the absence of any significant stereocontrol from the yttrium catalyst over these large, seven-membered substituted ϵ -caprolactones. This latter lack of stereocontrol is assumed to arise from a too long range between adjacent chiral centers, preventing an effective chain-end stereocontrolled mechanism.

Received 27th March 2024,
Accepted 13th April 2024

DOI: 10.1039/d4py00330f
rsc.li/polymers

Introduction

The ring-opening polymerization (ROP) of cyclic esters is by now a well-established privileged synthetic method towards the synthesis of polyesters with controlled features and especially exhibiting tunable microstructures (in particular, tacticity).¹ To this end, one of the most effective series of catalysts relies on rare earth metal complexes, such as those supported by achiral tripodal dianionic diamino- or amino-alkoxy-

bisphenolate ligands $\{ON(X)O^{R2}\}^{2-}$ ($X = NMe_2, OMe$; $R = o,p$ -substituents on phenolates).² These achiral complexes, associated with an exogeneous alcohol as a co-initiator, have been extensively studied with a wide range of monomers, displaying high activities and high degrees of control (molar mass, dispersity, end-group fidelity, tacticity *etc.*).

One of the ubiquitous illustrations of this chemistry is the stereoselective ROP of six-membered lactides.^{1,3} The ROP of racemic lactide (*rac*-LA) mediated by achiral yttrium $Y\{ON(N)O^{R2}\}$ complexes bearing sterically bulky substituents on the ancillary phenolate ligand ($R = tBu$, adamantyl, CMe_2Ph , CMe_2tBu , CPh_3) returns highly heterotactic PLA (P_r up to 0.96[†]) (Scheme 1). Also, the ROP of the four-membered β -butyrolactone (*rac*-BPL^{Me}) mediated by the related $Y\{ON(X)O^{R2}\}$

^aUniv. Rennes, CNRS, Institut des Sciences Chimiques de Rennes, UMR 6226, F-35042 Rennes, France. E-mail: sophie.guillaume@univ-rennes.fr, jean-francois.carpentier@univ-rennes.fr

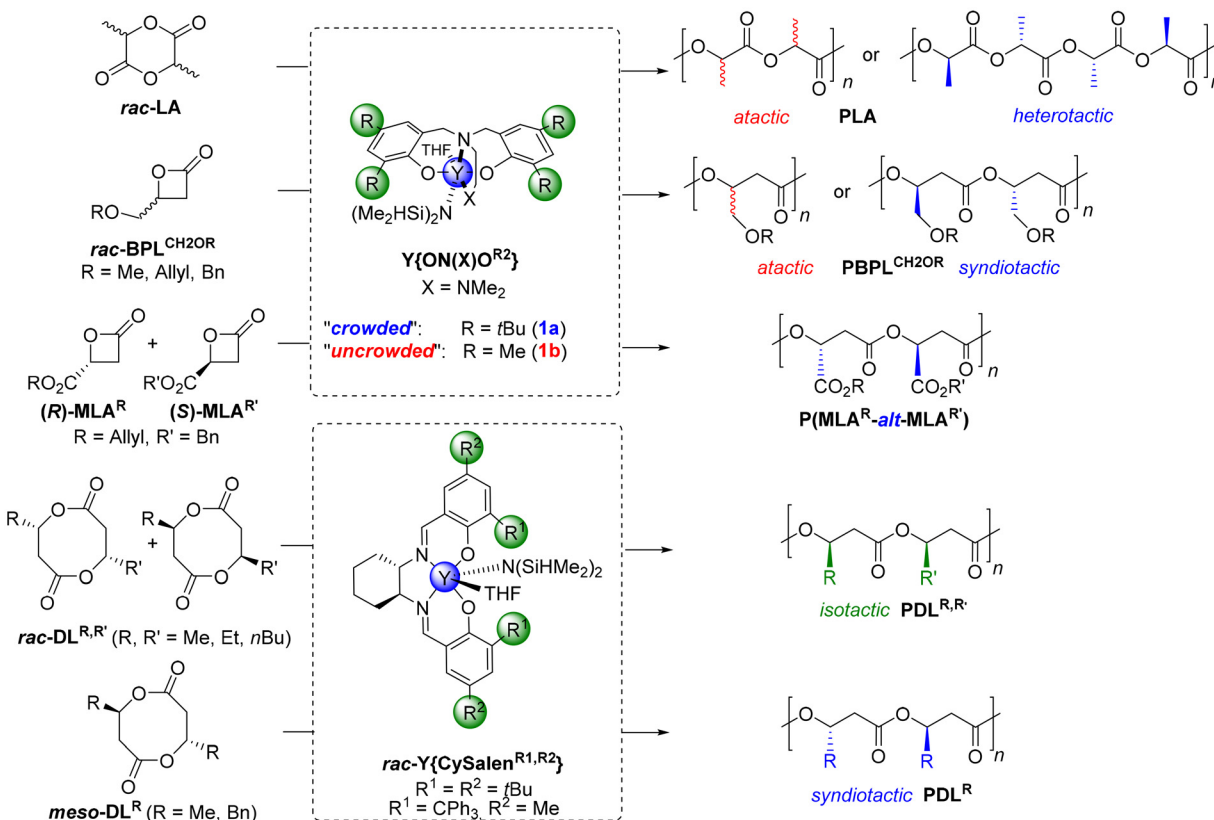
^bUniv. Rennes, Centre Régional de Mesures Physiques de l'Ouest, UAR 2025 ScanMAT, F-35042 Rennes, France

^cUniv. Libanaise, Campus Universitaire Rafic Hariri Hadath, Faculté des Sciences, Laboratoire de Chimie Médicinale et des Produits Naturels, Beirut, Lebanon

† Electronic supplementary information (ESI) available. See DOI: <https://doi.org/10.1039/d4py00330f>

[†] $P_{r/m}$ is the probability of *racemo/meso* enchainment between adjacent monomer units, as determined by ¹³C NMR spectroscopy, with $P_r + P_m = 1$; $P_r = 1$ for a perfectly syndiotactic polymer, $P_r = P_m = 0.5$ for an atactic one, and $P_m = 1$ for a perfectly isotactic polymer.





Scheme 1 Examples of yttrium-mediated stereoselective ROP/ROCOP of *rac*-lactide, *rac*-4-substituted- β -propiolactones, β -malolactones, or *rac*-diolides.^{3,6,9,10}

yttrium catalysts proceeds with high activities and enables fine-tuning of the microstructure of the resulting poly(3-hydroxybutyrate)s (poly(BPL^{Me}), aka PHB) from atactic to highly syndiotactic (P_r up to 0.96 \ddagger), depending on the nature of the *ortho*- (and to a much lesser extent the *para*-) R substituents on the tripodal ligand.^{4,5} Similarly, the ROP of four-membered 4-alkoxymethylene-substituted β -propiolactones, *rac*-BPL^{CH₂OR (R = Me, All, Bn), offers syndiotactic poly(BPL^{CH₂OR}) (P_r up to 0.91 \ddagger) provided sterically crowded *tert*-butyl, cumyl or trityl substituents are installed on the yttrium complexes, or atactic poly(BPL^{CH₂OR}) with non-crowded complexes bearing methyl-substituted ligands. More uniquely, the corresponding achiral halogen-substituted yttrium catalysts Y{ON(X)O^{Z2}} (Z = F, Cl, Br) give highly isotactic poly(BPL^{CH₂OR})s (P_m up to 0.95 \ddagger), thanks to attractive non-covalent interactions (NCIs) between the ligand halogen and the acidic methylene hydrogens within the growing polymer chain (Scheme 1).^{6,7} Also, using a syndioselective catalyst, the ROP of equimolar mixtures of two different, enantiomerically pure 4-substituted- β -propiolactones, with opposite configurations, gives highly alternating polyhydroxyalkanoates (PHAs).⁸ For instance, the ROP of enantiopure allyl (*S*)- β -malolactone and benzyl (*R*)- β -malolactone (MLA^R; R' = allyl, benzyl) (1:1), using a Y{ON(X)O^{R2}} yttrium catalyst bearing bulky R substituents, returns a nearly perfectly alternating copolymer, poly(MLA^{Allyl}-alt-MLA^{Benzyl}) (Scheme 1).⁹ In another related approach to}

form microstructurally controlled PHAs, chiral salen-yttrium catalysts have been used by the group of Chen for the stereoselective ROP of alkyl-substituted eight-membered racemic cyclic diolides (*rac*-DL^R).¹⁰ Hence, the ROP of *rac*-DL^{Me} proceeds readily to offer perfectly isotactic poly(DL^{Me}), that is, PHB (P_m up to 0.99 \ddagger) with a controlled and high molar mass (M_n up to 154 000 g mol⁻¹, D_M = 1.01). Similarly, starting from unsymmetrical disubstituted eight-membered diolides *rac*-DL^{R,R'} (R ≠ R') or by copolymerizing *rac*-DL^{Me} with *rac*-DL^{R'} (R' = Et, nBu), highly alternating isotactic poly(DL^{R,R'})s were produced (P_m up to 0.99 \ddagger). Access to syndiotactic PHAs (P_r up to 0.88 \ddagger) was also accomplished starting from *meso*-DL^R (Scheme 1).¹⁰

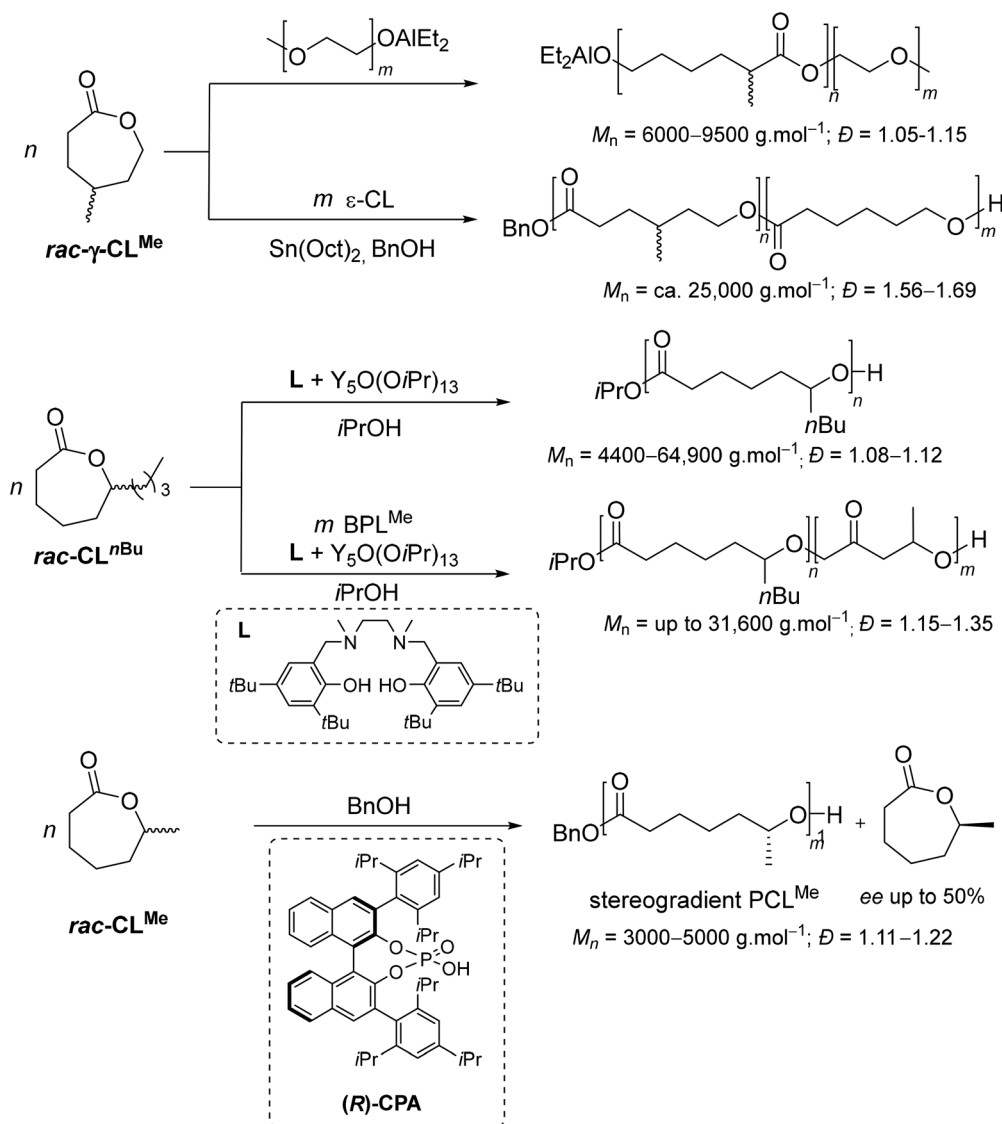
On the other hand, poly(ϵ -caprolactone) (PCL) is another quite important polyester,¹¹ first synthesized by Carothers' group in the 1930s from the parent seven-membered lactone (CL).¹² PCL is semi-crystalline (up to 70% depending on the weight-average molar mass, M_w) with a low melting point (59–60 °C); it is hydrophobic with good solubility, features exceptional blending compatibility, and shows good degradation abilities by microorganisms¹³ – a set of distinctive properties making it extensively valuable in different application fields. The ROP of CL and its alkyl-substituted derivatives such as 1-methyl- ϵ -caprolactone (CL^{Me}), mediated either by metal-based or organo-catalysts, has been the method of choice to target PCL-type materials and related copolymers, with



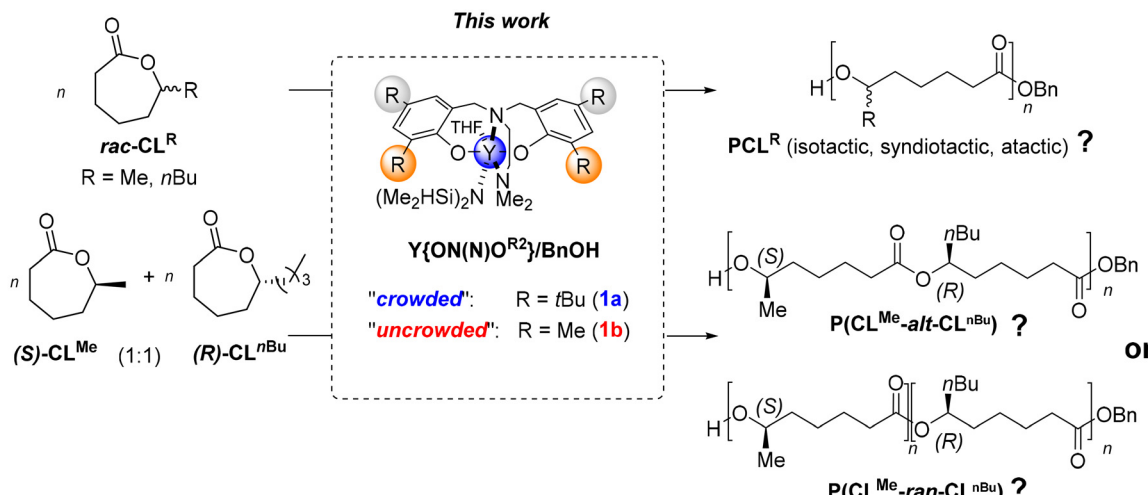
minimum backbiting and obtaining very high molar mass PCL (M_n up to 730 000 g mol⁻¹) with a narrow dispersity ($D \sim 1.1$) (Scheme 2).¹⁴ For instance, γ -methyl- ϵ -caprolactone has been polymerized using an ω -hydroxy-poly(ethylene oxide) macroinitiator combined with triethylaluminium,¹⁵ or copolymerized with CL using tin(II) bis(2-ethylhexanoate).¹⁶ Recently, the ROP of a series of spirocyclic acetal-functionalized ϵ -caprolactone monomers with zinc- or yttrium-based catalysts has been shown to open the route towards readily depolymerizable (*i.e.*, chemically recyclable) materials.¹⁷ The ring-opening copolymerization (ROCOP) of β -butyrolactone (BPL^{Me}) and 1-*n*-butyl- ϵ -caprolactone (that is ϵ -decalactone, hereafter referred to as CL^{*n*Bu}) mediated by yttrium-salan-type complexes, forms di- and triblock copolymers (M_n up to 31 600 g mol⁻¹, $D = 1.15\text{--}1.35$).¹⁸ Also, CL^{Me} has been homopolymerized using chiral phosphoric acids (CPAs), in kinetic resolution polymerizations, affording stereogradient PCL^{Me} with a high chain-end

fidelity and controlled molar mass (M_n up to 5000 g mol⁻¹, $D = 1.11\text{--}1.22$).¹⁹ The microstructure of the synthesized PCL^{Me} was determined using chiral HPLC to assess the enantiomeric excess (ee) values of the unreacted CL^{Me} monomer at various conversion levels, revealing that (*S*)-CPA consumes (*S*)-CL^{Me} faster while (*R*)-CPA polymerizes (*R*)-CL^{Me} preferentially. Yet, despite the progress made in polymerizing substituted ϵ -caprolactones, determination of the microstructure of the resulting materials has remained a challenge. In fact, the tacticity of these polymers could not be successfully assessed from their ¹H and ¹³C NMR spectra. It was suggested to arise from the chiral centers along the polymer backbone that are positioned too far apart to allow a clear differentiation by NMR analysis, and from an insufficient resolution of resonances even at 125 MHz.^{18,19}

In our study, we aimed at investigating the stereoselective ability of achiral yttrium catalysts of the type Y{ON(N)O^{R2}} in



Scheme 2 Examples of RO(CO)P of substituted- ϵ -caprolactones.^{15,16,18,19}



Scheme 3 ROP of 1-substituted- ϵ -caprolactones ($rac\text{-CL}^R$; $R = \text{Me, } n\text{Bu}$) and ROCOP of equimolar mixtures of opposite-configuration, enantiopure monomers studied in the present work to assess the stereoselectivity ability of discrete yttrium complexes towards such seven-membered lactones.

the RO(CO)P of the seven-membered 1-substituted- ϵ -caprolactones, namely CL^{Me} and $\text{CL}^{n\text{Bu}}$ (Scheme 3). Conventionally, the tacticity of polyesters is determined through NMR spectroscopy, enabling us to infer the extent, and sometimes also to decipher the mechanism, of stereocontrol. However, as mentioned earlier and further documented in the present work, since NMR spectroscopy proved ineffective in assessing the tacticity in the PCL^R homopolymers ($R = \text{Me, } n\text{Bu}$) resulting from these large lactones, we implemented an alternative approach. This involved copolymerizing equimolar mixtures of the two enantiomerically pure, opposite-configuration 1-substituted- ϵ -caprolactones $(S)\text{-CL}^{\text{Me}}$ and $(R)\text{-CL}^{n\text{Bu}}$, to investigate whether or not there is alternation of the monomer units in the resulting copolymers. Such alternation would be a hallmark of syndiotactic control (*vide infra*).^{8,9} For this purpose, because NMR spectroscopy eventually turned out to be uninformative to assess the degree of alternation/randomness in the synthesized poly[$(S)\text{-CL}^{\text{Me}}/(R)\text{-CL}^{n\text{Bu}}$] copolymers, extensive high resolution mass spectrometry (MS) analyses were conducted. With the aid of programmatic script, these MS studies enabled us to conclude on the stereoselective abilities of $\text{Y}\{\text{ON}(\text{N})\text{O}^{R^2}\}$ in the ROP of such 1-substituted- ϵ -caprolactones.

Experimental section

Materials and methods

All manipulations involving organometallic catalysts were performed under an inert atmosphere (argon, <5 ppm O_2 and H_2O) using standard Schlenk, vacuum line, and glovebox techniques. Toluene was freshly distilled from Na/benzophenone under argon and degassed thoroughly by freeze-thaw-vacuum cycles prior to use. Benzyl alcohol (BnOH) was distilled over Mg turnings under an argon atmosphere and kept over activated 3–4 \AA molecular sieves. Proligands $\{\text{ON}(\text{N})\text{O}^{t\text{Bu}2}\}\text{H}_2$ and $\{\text{ON}(\text{N})\text{O}^{\text{Me}2}\}\text{H}_2$ and precursor $\text{Y}[\text{N}(\text{SiHMe}_2)_2]_3(\text{THF})_2$, used to

prepare *in situ* yttrium amido complexes **1a–b**, respectively, were synthesized according to the reported procedures.^{4b,20} Racemic ϵ -decalactone ($rac\text{-CL}^{n\text{Bu}}$) was purchased from Sigma Aldrich and dried over CaH_2 .

Instrumentation and measurements

^1H (500 and 400 MHz) and $^{13}\text{C}\{^1\text{H}\}$ (125 and 100 MHz) NMR spectra were recorded on Bruker Avance Ascend 400 spectrometers at 25 $^\circ\text{C}$. ^1H and $^{13}\text{C}\{^1\text{H}\}$ NMR spectra were referenced internally relative to SiMe_4 ($\delta = 0$ ppm) using the residual solvent resonances. Coupling constants are reported in Hz.

The number-average molar mass ($M_{n,\text{SEC}}$) and dispersity ($D_M = M_w/M_n$) values of the PCL^R ($R = \text{Me, } n\text{Bu}$) homopolymer and copolymer samples were determined by size-exclusion chromatography (SEC) in THF at 30 $^\circ\text{C}$ (flow rate = 0.8 mL min $^{-1}$) on a Polymer Laboratories PL50 apparatus equipped with a refractometric detector and a UV detector at 254 nm, and a set of two ResiPore PLgel 3 μm MIXED-D 300 \times 7.5 mm columns. The (co)polymer samples were dissolved in THF (5 mg mL $^{-1}$). All elution curves were calibrated with polystyrene standards; the $M_{n,\text{SEC}}$ values of the PCL^R samples were uncorrected for the possible difference in the hydrodynamic radius *vs.* that of polystyrene. Representative SEC traces are given in the ESI as Fig. S26 and S27.†

The molar mass of PCL^R samples was also determined by ^1H NMR analysis in CDCl_3 from the relative intensities of the signals of the PCL^R repeating unit methine hydrogen (δ 4.84–4.90 ppm), $-\text{OCH}((\text{CH}_2)_4\text{CH}(\text{R}))$ and the benzyloxy chain-end (δ 5.09–5.11 ppm, $-\text{OCH}_2\text{Ph}$). The accuracy of the $M_{n,\text{NMR}}$ values thus determined is evaluated to be ± 200 g mol $^{-1}$. Monomer conversions were calculated from the ^1H NMR spectra of the crude polymer samples in CDCl_3 by using the integration (Int.) ratios $[\text{Int.}^{\text{R}}_{\text{PCL}}/(\text{Int.}^{\text{R}}_{\text{PCL}} + \text{Int.}^{\text{R}}_{\text{CL}})]$ of the methine hydrogens of PCL^R (*vide supra*) and of the monomers (δ 4.32 ppm, CL^{Me} ; δ 4.17 ppm, $\text{CL}^{n\text{Bu}}$).



Matrix Assisted Laser Desorption Ionization-Time of Flight (MALDI-ToF) high resolution (error <25 ppm) mass spectra were recorded using an ULTRAFLEX III TOF/TOF spectrometer (Bruker Daltonik GmbH, Bremen, Germany) in positive ionization mode at CRMPO, ScanMat, Université de Rennes. Spectra were recorded using reflectron mode and an accelerating voltage of 25 kV. A mixture of a freshly prepared solution of the polymer in CH_2Cl_2 (HPLC grade, 10 mg mL^{-1}) and DCTB (*trans*-2-(3-(4-*tert*-butylphenyl)-2methyl-2-propenylidene)-malononitrile, and an acetonitrile solution of the cationizing agent ($\text{CF}_3\text{CO}_2\text{Na}$ or NaI , 10 mg mL^{-1}) were prepared. The solutions were combined in a 1:1:1 v/v ratio of matrix-to-sample-to-cationizing agent. The resulting solution (0.25–0.5 μL) was deposited onto the sample target (entry 1: Prespotted AnchorChip PAC II 384/96 HCCA; entry 3: MTP 384 ground steel) and air- or vacuum-dried.

Electrospray Ionization (ESI) high resolution (error <3 ppm) mass spectra were recorded using an Orbitrap Q-Exactive spectrometer (Thermo Fisher Scientific, Waltham (MA), USA) in positive ionization mode at CRMPO, ScanMat, Université de Rennes. The sample was dissolved in MeOH before being analyzed by direct injection.

Differential scanning calorimetry (DSC) analyses were performed on a DSC 2500 TA instrument calibrated with indium using aluminum capsules (40 μL). The thermograms were recorded under a continuous flow of helium (25 mL min^{-1}) according to the following cycles: –80 to +200 $^{\circ}\text{C}$ at 10 $^{\circ}\text{C min}^{-1}$; +200 to –80 $^{\circ}\text{C}$ at 10 $^{\circ}\text{C min}^{-1}$; –80 $^{\circ}\text{C}$ for 5 min; –80 to +200 $^{\circ}\text{C}$ at 10 $^{\circ}\text{C min}^{-1}$; +200 to –80 $^{\circ}\text{C}$ at 10 $^{\circ}\text{C min}^{-1}$. Representative DSC traces of homo- and copolymers are reported in the ESI as Fig. S28–S36.†

Program for automatic assignment of m/z peaks in HRMS spectra

A program was developed to process the high-resolution mass spectroscopy data of $\text{P}(\text{CL}^{\text{Me}}\text{-}co\text{-}\text{CL}^{n\text{Bu}})$ copolymers, in order to establish the correspondence between the experimentally measured and theoretical m/z values, based on the measurement precision. The program supports as input Excel csv files representing the list of peaks (m/z and intensity), and aims to create: (a) as an *in silico* or real output, the table of calculated m/z values with the corresponding A_xB_y chemical formula (where A and B refer to the two comonomers), population type, and x and y values, and (b) as an output file, the table of measured m/z values and intensity of the MS peaks. The table of theoretical values (mono-isotopic exact masses) is generated from the different raw formulae (with different possible end-groups or as cyclic species) using the in-house software *Polymers* (see Fig. S15 in the ESI†), by considering some relevant MS parameters (ionization mode, polarity, type of adducts and charge state). The table of measured m/z values compiles the list of the peaks of the spectrum extracted using the *Vendor* software for each MS spectrum. The algorithm next determines the correspondence between the measured and the theoretical m/z values according to a measurement precision criterion expressed in ppm, as configured in the script; the measure-

ment precision criterion can be set at 3 ppm, for the analysis of ESI HR-MS data, and 30 ppm for MALDI-ToF HR-MS data. When several matches are possible, only the closest one is kept. A table of results is automatically generated allowing the correspondence between the theoretical and measured m/z values to be recorded with their relative intensity and measurement precision. As output, the software also takes into account the theoretical isotope contributions and delivers a summation of intensities for the measured m/z values respecting the measurement precision criterion. Thus, one can interpret the spectrum according to the different compositions identified within each population considered and their corrected relative intensity.

Separation of the enantiomers of $rac\text{-}\text{CL}^{\text{Me}}$ and $rac\text{-}\text{CL}^{n\text{Bu}}$ by preparative chiral HPLC analyses

This was performed at Institut des Sciences Moléculaires de Marseille, Plateforme de chromatographie chirale (UMR 7313 CNRS-University of Aix-Marseille, France), using Chiralpak AD-H (250 × 10 mm) columns, an Agilent 1260 Infinity unit (pump G1311B, autosampler G1329B, DAD G1315D), with Igloo-Gil ovens, monitored by SRA Instruments Seleccol software (Version 1.2.3.0), Agilent OpenLAB CDS Chemstation LC and CE Drivers (A.02.08SP1) and Agilent OpenLAB Intelligent reporting (A.01.06.111). Chiroptical detection was performed using a Jasco OR-1590 polarimetric detector. *n*-Heptane and iPrOH, HPLC grade, were degassed and filtered on a 0.45 μm millipore membrane before use. Chiral HPLC traces for racemic and enantiopure CL^{Me} and $\text{CL}^{n\text{Bu}}$ are reported in the ESI as Fig. S3 and S4.†

Determination of reactivity ratios following the Fineman–Ross method

Following reported procedures,²¹ the monomer reactivity ratios during the synthesis of the copolymers, r_1 and r_2 , were calculated using the Fineman–Ross equation:

$$F/(f(f-1)) = r_1(F^2/f) - r_2 \quad (1)$$

where $F = M_1/M_2$ (molar ratio of the comonomer feed composition) and $f = m_1/m_2$ (molar ratio of each segment within the recovered copolymer). The plot of this equation for a couple of data points (Fig. S10†) returned a straight line with the slope equal to r_1 and the intercept equal to $-r_2$.

Synthesis of *racemic* 1-methyl- ϵ -caprolactone ($rac\text{-}\text{CL}^{\text{Me}}$)

The synthesis of $rac\text{-}\text{CL}^{\text{Me}}$ was performed by the Baeyer–Villiger oxidation of 2-methylcyclohexanone, following a reported protocol^{10c} that provides 1-methyl- ϵ -caprolactone as a major compound (95%; along 5% of 5-methyl- ϵ -caprolactone): 2-methylcyclohexanone (9.0 g, 79.8 mmol) was dissolved in CH_2Cl_2 (100 mL); *m*-CPBA (27.5 g, 159.7 mmol) was added and the solution was stirred in the dark for 48 h at 0 $^{\circ}\text{C}$. A white suspension formed, which was filtered, and the filtrate was washed with a saturated aqueous NaHCO_3 solution (3 × 100 mL) followed by a 5wt% $\text{Na}_2\text{S}_2\text{O}_3$ solution (3 × 100 mL).



The organic phase was dried over Na_2SO_4 and evaporated. The crude product was purified by chromatography using basic alumina and hexanes as eluents to give $\text{rac-CL}^{\text{Me}}$ as a colorless liquid (6.4 g, 62%). $\text{rac-CL}^{\text{Me}}$ was further dried over CaH_2 , vacuum-distilled (94 °C, 5 mmHg) and stored under argon. ^1H NMR (400 MHz, CDCl_3 , 25 °C) (Fig. S1†): δ 1.20 (d, $^3J_{\text{H-H}} = 6.7$, 3H, CH_3CH), 1.43–1.53 (m, 3H, $\text{CHCH}_2\text{CH}_2\text{CH}_2$), 1.72–1.82 (m, 3H, $\text{CHCH}_2\text{CH}_2\text{CH}_2$), 2.44–2.51 (m, 2H, $\text{CH}_2\text{C}(\text{O})\text{O}$), 4.26–4.37 (m, 1H, CHCH_3). $^{13}\text{C}\{\text{H}\}$ NMR (100 MHz, CDCl_3 , 25 °C) (Fig. S2†): δ 22.2 (CH_3CH), 30.9 ($\text{CHCH}_2\text{CH}_2\text{CH}_2$), 33.3 ($\text{CHCH}_2\text{CH}_2\text{CH}_2$), 35.4 ($\text{CHCH}_2\text{CH}_2\text{CH}_2$), 37.4 ($\text{CHCH}_2\text{CH}_2\text{CH}_2$), 68.2 ($\text{CH}_2\text{C=O}$), 176.1 (C=O).

Typical procedure for the ROP of rac-CL^{R}

In a typical experiment, in the glovebox, a Schlenk flask was charged with $\text{Y}[\text{N}(\text{SiHMe}_2)_2]_3(\text{THF})_2$ (8.8 mg, 14 μmol) and $\{\text{ON}(\text{N})\text{O}^{\text{tBu}2}\}\text{H}_2$ (7.4 mg, 14 μmol), and toluene (0.25 mL) was next added. To this solution, BnOH (107 μL of a 1% v/v solution in toluene, 1 equiv. vs. Y) was added under stirring at room temperature. After 5 min, a solution of $\text{rac-CL}^{\text{Me}}$ (150 mg, 0.84 mmol, 60 equiv. vs. Y) in toluene (0.5 mL) was added rapidly and the mixture was stirred at 20 °C for 1 h. The reaction was quenched by the addition of acetic acid (ca. 0.5 mL of a 1.6 mol L⁻¹ solution in toluene). The mixture was concentrated to dryness under vacuum and the conversion was determined by the ^1H NMR analysis of the residue in CDCl_3 . The crude polymer was then dissolved in CH_2Cl_2 (ca. 1 mL) and precipitated in cold pentane (ca. 5 mL), filtered and dried in a vacuum oven at 60 °C. The homopolymers were recovered as pale yellowish oils.

PCL^{Me}. ^1H NMR (400 MHz, CDCl_3 , 25 °C) (Fig. S5†): δ 7.34 (broad m, 5H, $\text{C}_6\text{H}_5\text{CH}_2\text{O}$), 5.11 (s, 2H, $\text{C}_6\text{H}_5\text{CH}_2\text{O}$), 4.90 (sext, $^3J_{\text{H-H}} = 6.2$, 1H, CHCH_3), 2.26 (t, $^3J_{\text{H-H}} = 7.6$, 2H, COCH_2-), 1.61, 1.48, and 1.33 (m, 6H, $\text{COCH}_2\text{CH}_2\text{CH}_2\text{CH}_2\text{CH}$), 1.19 (d, $^3J_{\text{H-H}} = 6.4$, 3H, CH_3). $^{13}\text{C}\{\text{H}\}$ NMR (100 MHz, CDCl_3 , 25 °C) (Fig. S6†): δ 173.2 (CO), 128.7, 128.4, 124.9, 123.4 (4s, $\text{C}_6\text{H}_5\text{CH}_2\text{O}$), 70.7 (CHCH_3), 66.3 ($\text{C}_6\text{H}_5\text{CH}_2\text{O}$), 35.7 (COCH_2), 34.6 ($\text{COCH}_2\text{CH}_2\text{CH}_2\text{CH}_2\text{CH}$), 25.2 and 25.1 ($\text{COCH}_2\text{CH}_2\text{CH}_2\text{CH}_2\text{CH}$), 20.1 (CH_3).

PCL^{nBu}. ^1H NMR (400 MHz, CDCl_3 , 25 °C) (Fig. S7†): δ 7.33 (broad m, 5H, $\text{C}_6\text{H}_5\text{CH}_2\text{O}$), 5.09 (s, 2H, $\text{C}_6\text{H}_5\text{CH}_2\text{O}$), 4.84 (pent, $^3J_{\text{H-H}} = 6.0$, 1H, $(\text{CH}_2)_4\text{CH}(\text{OH})(\text{CH}_2)_3\text{CH}_3$), 2.25 (t, $^3J_{\text{H-H}} = 8.0$, 2H, COCH_2) 1.60 (m, 2H, COCH_2CH_2) 1.50 (m, 4H, $\text{COCH}_2\text{CH}_2\text{CH}_2\text{CH}_2\text{CH}(\text{OH})\text{CH}_2$), 1.26 (m, 6H, $\text{CH}_2\text{CH}_2\text{CH}(\text{OH})\text{CH}_2\text{CH}_2\text{CH}_2\text{CH}_3$), 0.86 (t, $^3J_{\text{H-H}} = 6.8$, 3H, CH_3CH_2). $^{13}\text{C}\{\text{H}\}$ NMR (100 MHz, CDCl_3 , 25 °C) (Fig. S8†): δ 173.3 (CO), 128.6, 128.2, 124.9, 123.4 (4s, $\text{C}_6\text{H}_5\text{CH}_2\text{O}$), 73.9 (CH_-), 60.0 ($\text{C}_6\text{H}_5\text{CH}_2\text{O}$), 34.6 (COCH_2), 33.9 ($\text{CH}_2\text{CHCH}_2\text{CH}_2\text{CH}_2\text{CH}_3$), 27.6 ($\text{CHCH}_2\text{CH}_2\text{CH}_2\text{CH}_3$), 25.1 ($\text{COCH}_2\text{CH}_2\text{CH}_2\text{CH}_2\text{CH}$), 22.7 ($\text{CHCH}_2\text{CH}_2\text{CH}_2\text{CH}_3$), 14.1 (CH_3).

Typical procedure for the ROCOP of $(S)\text{-CL}^{\text{Me}}$ with $(R)\text{-CL}^{\text{nBu}}$

In a typical experiment, in the glovebox, a Schlenk flask was charged with $\text{Y}[\text{N}(\text{SiHMe}_2)_2]_3(\text{THF})_2$ (3.7 mg, 5.8 μmol) and $\{\text{ON}(\text{N})\text{O}^{\text{tBu}2}\}\text{H}_2$ (**1a**, 3.0 mg, 5.8 μmol), and toluene (0.25 mL) was next added. To this solution, BnOH (60 μL of a 1% v/v

solution in toluene, 1 equiv. vs. Y) was added under stirring at room temperature. After 5 min, a solution of $(S)\text{-CL}^{\text{Me}}$ (>98% ee, 37.8 mg, 0.29 mmol, 50 equiv. vs. Y) and $(R)\text{-CL}^{\text{nBu}}$ (>98% ee, 50.0 mg, 0.29 mmol, 50 equiv. vs. Y) in toluene (0.25 mL) was added rapidly and the mixture was stirred at 20 °C for 3 h. The reaction was quenched by the addition of acetic acid (ca. 0.5 mL of a 1.6 mol L⁻¹ solution in toluene). The mixture was concentrated to dryness under vacuum and the conversion was determined by the ^1H NMR analysis of the residue in CDCl_3 . The crude polymer was then dissolved in CH_2Cl_2 (ca. 1 mL) and precipitated in cold pentane (ca. 5 mL), filtered and dried. $\text{P}(\text{CL}^{\text{Me}}\text{-co-CL}^{\text{nBu}})$ copolymers were recovered as pale yellowish oils. ^1H NMR (400 MHz, CDCl_3 , 25 °C) (signals were labelled from a-a' to h, as shown in Fig. 2) (see also Fig. S9 in the ESI†): δ 7.34 (broad m, 5H, $\text{C}_6\text{H}_5\text{CH}_2\text{O}$, h), 5.11 (s, 2H, $\text{C}_6\text{H}_5\text{CH}_2\text{O}$, g), 4.86 (2 overlapping m, $^3J_{\text{H-H}} = 6.4$, 2H, CHCH_3 , e + e'), 2.28 (m, 4H, COCH_2 , a + a'), 1.61 (m, 6H, $\text{COCH}_2\text{CH}_2\text{CH}_2\text{CH}_2$ and $\text{OCOCH}_2\text{CH}_2\text{CH}_2\text{CH}_2$, d + d'), 1.50 (m, 4H, COCH_2CH_2 and $\text{OCOCH}_2\text{CH}_2$, b + b'), 1.30 (m, 8H, $\text{CH}_2\text{CH}_2\text{CHCH}_2\text{CH}_2\text{CH}_2\text{CH}_3$ and $\text{OCOCH}_2\text{CH}_2\text{CH}_2\text{CH}_2$, c + c'), 1.19 (d, $^3J_{\text{H-H}} = 6.8$, 3H, CH_3 , f), 0.89 (t, $^3J_{\text{H-H}} = 7.1$, 3H, CH_3 , f). $^{13}\text{C}\{\text{H}\}$ NMR (100 MHz, CDCl_3 , 25 °C) (signals were labelled from #1 to #12, as shown in Fig. 3) (see also Fig. S10 in the ESI†): δ 173.4 (CO, #3), 173.2 (CO, #3'), 129.2, 128.4, 124.9, 123.5 (4s, $\text{C}_6\text{H}_5\text{CH}_2\text{O}$, #1), 74.0 ($\text{C}(\text{O})\text{OCHCH}_2$, #8), 70.7 (OCHCH_2 , #8'), 66.1 ($\text{C}_6\text{H}_5\text{CH}_2\text{O}$, #2), 35.7 (COCH_2 , #4 and #4'), 34.6 ($\text{CH}_2\text{CH}_2\text{CHOC}(\text{O})$, #7, and $\text{CHCH}_2(\text{CH}_2)\text{CH}_3$, #9), 33.9 ($\text{OCH}(\text{CH}_3)\text{CH}_2$, #7'), 27.6 ($\text{CHCH}_2\text{CH}_2\text{CH}_2\text{CH}_3$, #10), 25.1 (several signals, $\text{C}(\text{O})\text{CH}_2\text{CH}_2\text{CH}_2\text{CH}_2\text{CH}$, #5, #6, and $\text{OC}(\text{O})\text{CH}_2\text{CH}_2\text{CH}_2\text{CH}_2\text{CH}$, #5', #6'), 21.7 (s, $\text{CH}_3\text{CH}_2\text{CH}_2$, #11), 20.1 (CH_3CH , #9'), 14.1 ($\text{CH}_3\text{CH}_2\text{CH}_2$, #12).

Results and discussion

Homopolymerization of rac-CL^{R}

First, the homopolymerization of both $\text{rac-CL}^{\text{Me}}$ and $\text{rac-CL}^{\text{nBu}}$ was studied using the yttrium catalytic system $\{\text{ON}(\text{N})\text{O}^{\text{tBu}2}\}$ (**1a**)/ BnOH (Scheme 3), selected as a benchmark system considering its typical high productivity, activity and syndiotactic abilities toward a number of racemic 4- and 6-membered lactones (*vide supra*).^{2–7,9} The ROP reactions proceeded readily in toluene at room temperature to form the corresponding PCL^{Me} and PCL^{nBu} , respectively (Table S1†). The structures of the homopolymers were confirmed by ^1H and ^{13}C NMR spectroscopy (see the ESI, Fig. S3–S6†), indicating linear macromolecules capped with benzyloxycarbonyl and hydroxy end-groups. However, a close examination of the different signals in the ^{13}C NMR spectra did not allow establishing the polymer tacticity as anticipated (Fig. 1). As mentioned earlier, this is in line with previous literature reports, which stated that no differentiated *meso/racemo* diad sequences are observable in the ^{13}C NMR spectra of PCL^{R} s recorded at a 100–125 MHz field.^{18,19} To further confirm this observation, two quite different benchmark ROP catalytic systems, namely $\{\text{BDI}^{\text{DIPP}}\}\text{Zn}(\text{N}(\text{SiMe}_3)_2)/\text{BnOH}$ (hereafter referred to as $\text{Zn}\{\text{BDI}\}/\text{BnOH}$)²²



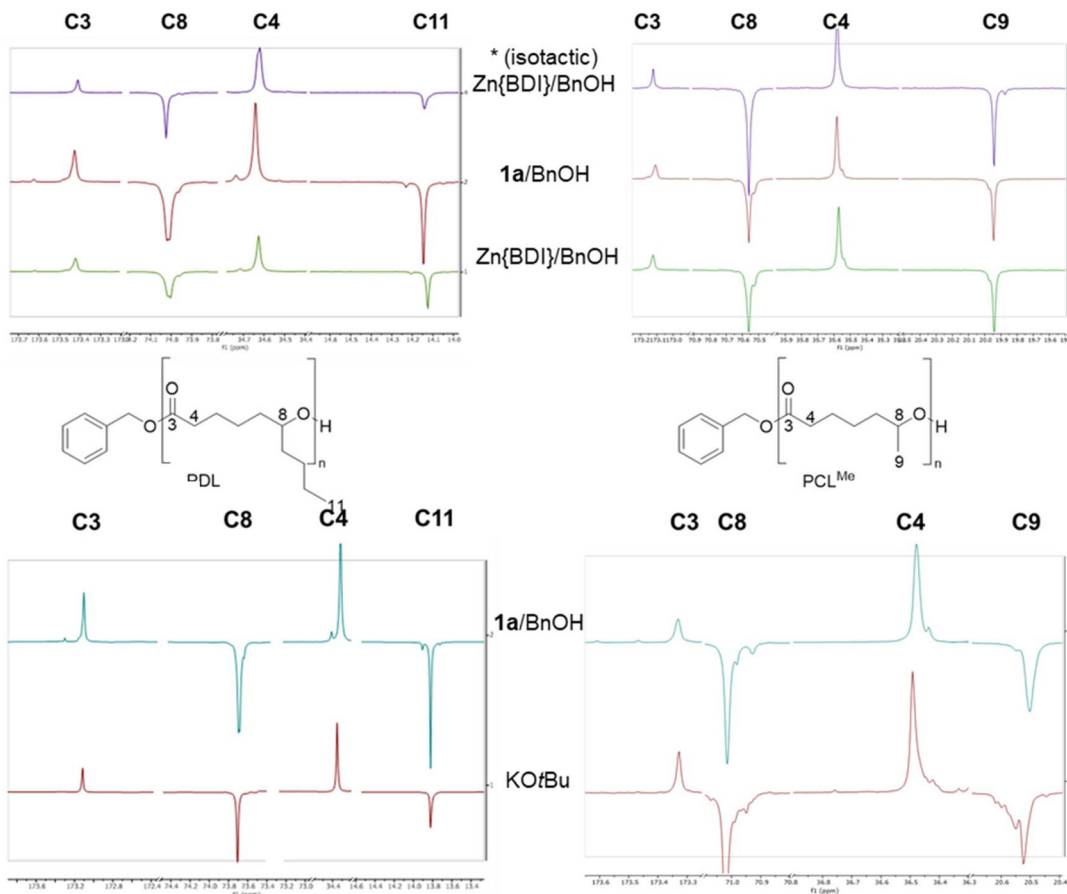


Fig. 1 Zoomed regions of the $^{13}\text{C}\{^1\text{H}\}$ NMR spectra (100 MHz, CDCl_3 (top) and $(\text{CD}_3)_2\text{CO}$, 25 °C) of $\text{PCL}^{n\text{Bu}}$ (left) and PCL^{Me} (right) homopolymers prepared by the ROP of $\text{rac-CL}^{\text{Me}}$ and $\text{rac-CL}^{n\text{Bu}}$, respectively, except for the spectra labeled (*), prepared from enantiopure $(S)\text{-CL}^{\text{Me}}$ and $(R)\text{-CL}^{n\text{Bu}}$, respectively, mediated by the $\{\text{Zn}(\text{BDI}^{\text{DIPP}})\}\text{Zn}(\text{N}(\text{SiMe}_3)_2)/\text{BnOH}$ system (Table S1,† entries 1–4). The low intensity signals observed are assigned to the terminal repeating units in these low molar mass polymers.

and potassium *tert*-butoxide, were used for comparison purposes (Table S1,† entries 2 and 3). Also, isotactic homopolymers ($P_m > 0.98$) were prepared starting from the enantiopure $(R)\text{-CL}^{\text{Me}}$ and $(R)\text{-CL}^{n\text{Bu}}$ monomers, respectively (preliminarily obtained by preparative chiral HPLC; see the Experimental section), using the $\{\text{BDI}^{\text{DIPP}}\}\text{Zn}(\text{N}(\text{SiMe}_3)_2)/\text{BnOH}$ system (Table S1,† entry 4). This eventually ended up with a set of PCL^{Me} and $\text{PCL}^{n\text{Bu}}$ homopolymers, with obviously different tacticities, whose ^{13}C NMR spectra yet were virtually identical and indistinguishable from those of polymers produced by $\text{Y}\{\text{ON}(\text{N})\text{O}^{\text{tBu}2}\}$ (**1a**). This absence of differentiated, observable *meso*/*racemo* diad sequences in the ^{13}C NMR spectra of PCL^{R} -type polymers is likely due to the long-range separation from one chiral group to the next one, despite the short (two bonds) distance between the chiral groups and the carbonyl groups. Note that all polymers featured essentially the same thermal signature (as determined by DSC; see the ESI, Fig. S28–S36†).²³

Copolymerization of $(S)\text{-CL}^{\text{Me}}$ with $(R)\text{-CL}^{n\text{Bu}}$

An alternative way to assess the stereoselective ability of achiral $\text{Y}\{\text{ON}(\text{X})\text{O}^{\text{R}2}\}$ catalysts towards racemic 1-substituted ϵ -caprolactones is through the investigation of the ROCOP of 1:

1 mixtures of two chemically different, enantiopure CL^{R} monomers with opposite configurations. Indeed, with such comonomer feed, (highly) syndioselective catalysts shall return (highly) alternating copolymers (as previously demonstrated with various chiral β -lactones and $\text{Y}\{\text{ON}(\text{X})\text{O}^{\text{R}2}\}$ -type catalysts);^{8,9} on the other hand, (highly) isoselective catalysts shall provide (highly) blocky copolymers, while non-stereoselective catalysts shall give random copolymers. This is, of course, assuming that both monomers have essentially the same reactivity/polymerizability, that is, the reaction is under stereocontrol rather than being governed by kinetic considerations. This is anticipated in the present case because of the limited stereoelectronic difference in the R substituents (*i.e.*, Me vs. $n\text{Bu}$) of the two CL^{R} monomers.²⁴ Finally, it is expected that examining the comonomer sequence (alternation/randomness degree) in the resulting polycaprolactone copolymers would be easier than assessing tacticity in the corresponding homopolymers.

Hence, the ROCOP of 1:1 mixtures of $(S)\text{-CL}^{\text{Me}}$ and $(R)\text{-CL}^{n\text{Bu}}$ was conducted with relatively low-to-moderate targeted molar mass ($M_n = \text{ca. } 3000 \text{ g mol}^{-1}$, DP = 20 up to $M_n = \text{ca. } 11\,000 \text{ g mol}^{-1}$, DP = 100), using either the **1a** or **1b** catalyst. The results are gathered in Table 1. The ^1H and ^{13}C NMR

Table 1 ROCOP of 1:1 mixtures of (S)-CL^{Me} and (R)-CL^{nBu} mediated by the **1a–b**/BnOH catalytic systems^a

Entry	Cat.	$[(S)\text{-CL}^{\text{Me}}]_0/[(R)\text{-CL}^{\text{nBu}}]_0/$ [BnOH] ₀	Reaction time ^b (min)	$[(S)\text{-CL}^{\text{Me}}]_0/[(R)\text{-CL}^{\text{nBu}}]_0$ Conv. ^c (%)	$M_{\text{n, theo}}^d$ (g mol ⁻¹)	$M_{\text{n,NMR}}^e$ (g mol ⁻¹)	$M_{\text{n,SEC}}^f$ (g mol ⁻¹)	D_{M}^f	T_{g}^g (°C)
1	1a	10:10:1	35	100:100	3100	3500	5500	1.17	-45.7
2	1a	10:10:1 ⁱ	40	100:100	3050	2900	4200	1.18	nd ^h
3	1a	10:10:1	390	100:100	3000	3100	4850	1.31	nd ^h
4	1a	50:50:1	180	100:86	10 400	9100	13 500	1.07	nd ^h
5	1a	50:50:1 ^j	300	100:97	15 200	10 000	11 500	1.11	nd ^h
6	1b	10:10:1	15 h 30	100:100	3100	3000	4150	1.27	-49.4
7	1b	28:33:1 ^k	300	63:46	4900	8600	5700	1.09	-59.8

^a Reactions performed with $[(S)\text{-CL}^{\text{Me}}]_0 = [(R)\text{-CL}^{\text{nBu}}]_0 = 1.0$ M in toluene with $[\text{1a–b}]/[\text{BnOH}]_0 = 1:1$. ^b Reaction time was not optimized.

^c Conversion of (S)-CL^{Me} and (R)-CL^{nBu} as determined by the ¹H NMR analysis of the crude reaction mixture. ^d Theoretical molar mass calculated according to $M_{\text{n, theo}} = [\text{CL}^{\text{Me}}]_0/[\text{1}] \times \text{conv.} (\text{CL}^{\text{Me}}) \times M(\text{CL}^{\text{Me}}) + [\text{CL}^{\text{nBu}}]_0/[\text{1}] \times \text{conv.} (\text{CL}^{\text{nBu}}) \times M(\text{CL}^{\text{nBu}}) + M(\text{BnOH})$, with $M(\text{CL}^{\text{Me}}) = 128$ g mol⁻¹, $M(\text{CL}^{\text{nBu}}) = 170$ g mol⁻¹ and $M(\text{BnOH}) = 108$ g mol⁻¹. ^e Molar mass as determined by the ¹H NMR analysis of the isolated polymer, from the resonances of the terminal OBr group (refer to the Experimental section). ^f Number-average molar mass (uncorrected) and dispersity ($M_{\text{w}}/M_{\text{n}}$) as determined by SEC analysis in THF at 30 °C vs. polystyrene standards. ^g Glass transition temperature as determined by DSC; no melting transition was observed. ^h Not determined. ⁱ Reaction performed with (R)-CL^{Me} and (S)-CL^{nBu}. ^j Reaction performed with *rac*-CL^{Me} and *rac*-CL^{nBu}. ^k Reaction performed using iPrOH as a co-initiator rather than BnOH.

spectra of the resulting copolymers (Fig. 2 and 3, respectively; see also the ESI, Fig. S9 and S10,† and the Experimental section) featured the characteristic resonances for the repeating units. Taking into account the benzyloxy end-group intro-

duced in the initiation step, the molar masses of the copolymers were calculated from the ¹H NMR spectra (see the Experimental section for calculation details). The $M_{\text{n,NMR}}$ values thus obtained were in good agreement with the $M_{\text{n, theo}}$

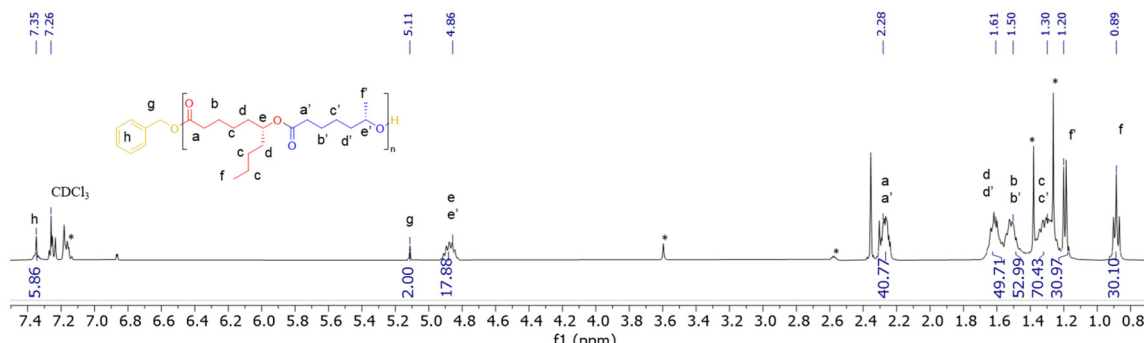


Fig. 2 Representative ¹H NMR spectrum (400 MHz, CDCl₃, 25 °C) of a P(CL^{Me}-co-CL^{nBu}) copolymer prepared from the ROCOP of a 1:1 mixture of (S)-CL^{Me} and (R)-CL^{nBu} mediated by the **1a**/BnOH (1:1) catalytic system (Table 1, entry 3). * stands for resonances of the residual solvent and/or catalyst.

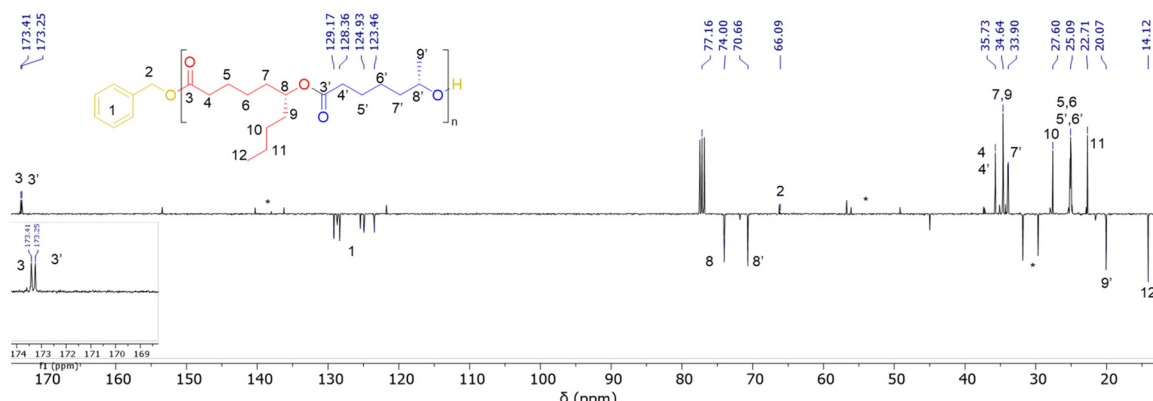


Fig. 3 Representative JMOD ¹³C{¹H} NMR spectrum (100 MHz, CDCl₃, 25 °C) of a P(CL^{Me}-co-CL^{nBu}) copolymer prepared from the ROCOP of a 1:1 mixture of (S)-CL^{Me} and (R)-CL^{nBu} mediated by the **1a**/BnOH (1:1) catalytic system (Table 1, entry 3). * stands for resonances of the residual solvent and/or catalyst.



values calculated from the monomer-to-initiator ratio and monomer conversion (Table 1). The $M_{n,SEC}$ values determined in chloroform *vs.* polystyrene standards (values uncorrected for possible differences in hydrodynamic radii) followed almost the same trend. The dispersity of the copolymers obtained was rather narrow, with D_M values ranging from 1.07 to 1.31. As

typical of this chemistry,^{2–6,8} the longer the reaction time, the greater the extent of transesterification reactions (reshuffling and back-biting), resulting in broadening of the dispersity (compare entries 1 and 2 *vs.* 3) (note that reaction times were not necessarily optimized in this study); this transesterification was further corroborated by mass spectrometric studies

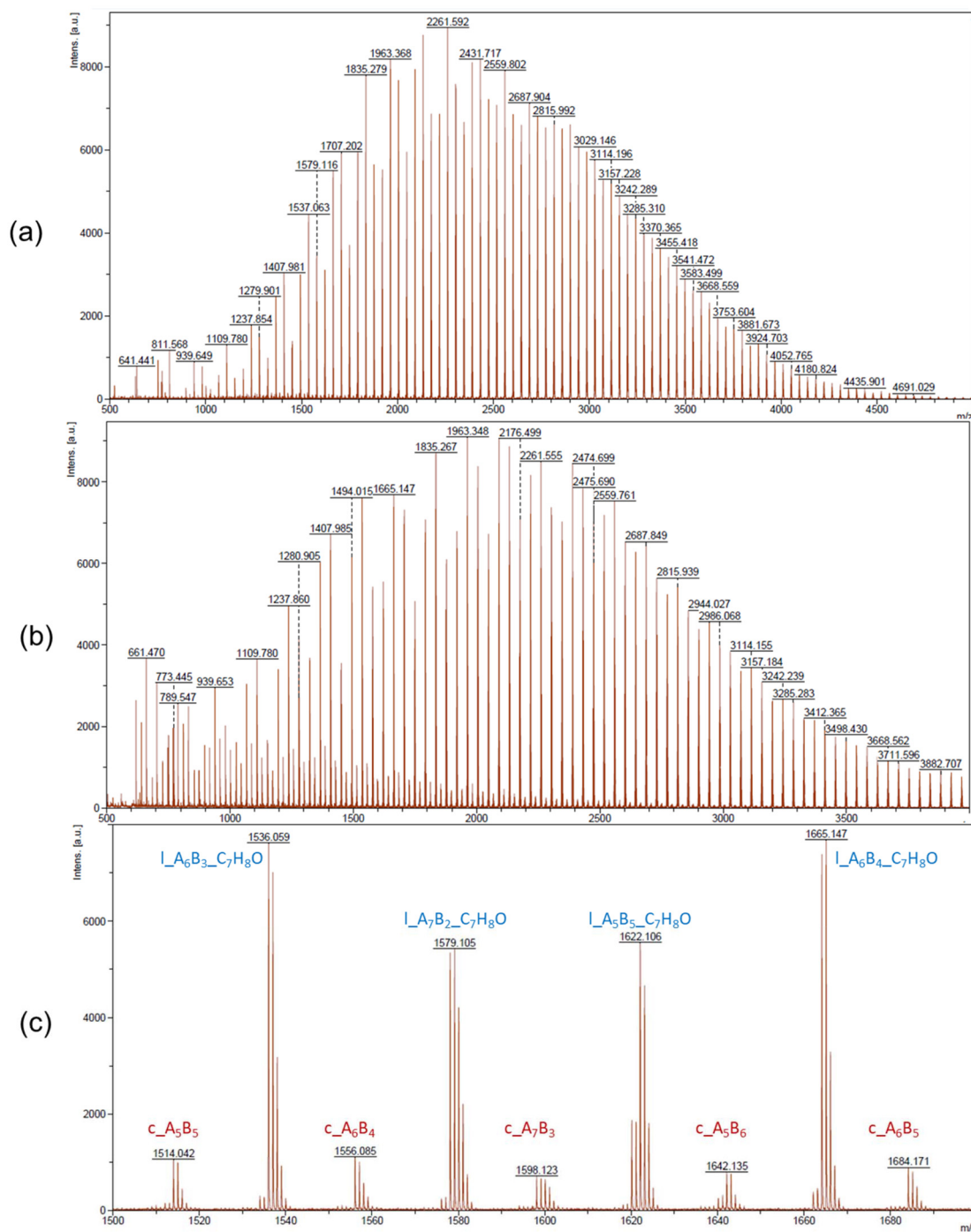


Fig. 4 MALDI-ToF mass spectra (DCTB matrix, ionized by Na^+) of $\text{P}(\text{CL}^{n\text{Bu}}\text{-co-CL}^{\text{Me}})$ copolymers prepared by the ROCOP of a 1:1 mixture of (R)- $\text{CL}^{n\text{Bu}}$ and (S)- CL^{Me} with the **1a**/BnOH catalytic system, over (a) 35 min and (b) 390 min, respectively (Table 1, entries 1 and 3, respectively) for m/z up to 4000, (c) zoomed region (m/z = 1500–1700) of the above MALDI-ToF mass spectrum (b) with corresponding assignments of the two major series observed. A_xB_y stands for x repeating units of A ($\text{CL}^{n\text{Bu}}$) and y repeating units of B (CL^{Me}) in $\text{P}(\text{CL}^{n\text{Bu}}\text{-co-CL}^{\text{Me}})$.

(*vide infra*). The reactions mediated by **1b** proceeded more slowly than those with **1a** (compare entries 4 and 5 vs. 7). This is a behavior previously noted in the ROP of different lactones² and accounted for by the likely aggregation of the sterically uncrowded **1b** in contrast to the mononuclear **1a** which is protected by *ortho*,*para*-*tert*-butyl substituents on the phenolate rings. Also, as mentioned earlier and anticipated considering the small increase in the substituent bulkiness, CL^{Me} appears to be slightly more reactive than CL^{nBu} (see entries 4, 5 and 7; for ^1H NMR monitoring see Fig. S11 in the ESI†).

Despite NMR spectroscopy confirming the formation of $\text{P}(\text{CL}^{\text{Me}}\text{-co-CL}^{\text{nBu}})$ copolymers, their detailed microstructure, in particular the alternation degree, could not be assessed using this technique. In fact, in the carbonyl region (C_3,C_3') and in the methine region (C_8,C_8') of all ^{13}C NMR spectra, only two resonances were observed that arose from the two chemically different CL^{Me} and CL^{nBu} monomer units (Fig. 3 and S10†); if ^{13}C NMR spectroscopy enables assessing alternation, more than two resonances would be observed, at least in the spectra of copolymers produced by catalyst **1b** since this one is notoriously poorly syndioselective, if not completely non-stereo-selective, due to its sterically small methyl substituents.⁹

Mass spectrometry (MS) is an alternative technique to NMR to study the sequence and microstructure of copolymers and, with proper data processing tools, more information concerning the composition, monomer sequence, polymer length, and reactivity ratios can be extracted.^{25–30} Hence, MS investigations were performed in order to better understand the microstructure of the $\text{P}(\text{CL}^{\text{Me}}\text{-co-CL}^{\text{nBu}})$ copolymers. Both MALDI-ToF and ESI mass spectra were recorded. One of the advantages of MALDI-ToF over ESI is that the range of m/z values of the returned mass spectra is greater; on the other hand, higher resolution can be often achieved with ESI.

In the MALDI-ToF mass spectra of our copolymers, the two major distributions observed featuring the most intense peaks refer to the linear $\alpha\text{-BnO},\omega\text{-OH-}[\text{P}(\text{CL}^{\text{nBu}})_x\text{-co-(CL}^{\text{Me}}\text{)}_y]$ and cyclic $[\text{P}(\text{CL}^{\text{nBu}})_x\text{-co-(CL}^{\text{Me}}\text{)}_y]$ series (Fig. 4 and S13–S14†). Similar observations were made from the ESI HR-mass spectra (Fig. 5).

and S16–S20†) from which both the aforementioned linear and cyclic populations could be unambiguously assigned.³¹ These MS data confirm the above NMR data regarding the formation of linear macromolecules with α -benzyloxy and ω -hydroxy end-groups. Noteworthily, cyclic populations cannot be assessed by NMR spectroscopy, since they have the same repeating units as linear chains, but no end-groups. The present observation of cyclic populations both in the MALDI-ToF and ESI mass spectra has two likely origins: (i) observation of cyclic macromolecules formed during the ROCOP process, arising from intramolecular back-biting/trans-esterification, as corroborated by the abovementioned broadening of the dispersities at longer reaction times, also in line being the MALDI-ToF mass spectrum of a copolymer prepared at short reaction time (35 min; Table 1, entry 1; Fig. 4a) features no cyclic population as compared to that of a copolymer exposed over a longer period to the catalytic system (390 min; Table 1, entry 3; Fig. 4b). (ii) Other possible reasons for the observation of a significant population of cyclic macromolecules by MALDI-ToF MS is likely the result of incidental over-expression of specific species during the crystallization process and/or the sample preparation for MS (in the acidic DCTB matrix, which promotes easy transesterification/cyclization).

For better depicting the distribution of different copolymer populations, assignments of the different series were established by the comparison of the experimental m/z values with the theoretical masses calculated for different copolymer compositions (*i.e.*, by varying the number of CL^{nBu} and CL^{Me} units for both values of x and y , along with the two different families indicated) (Table S2†). Fig. 6 depicts the distribution of each population thus obtained in two different $\text{P}(\text{CL}^{\text{nBu}}\text{-co-CL}^{\text{Me}})$ copolymers.

In our first attempts to determine the monomer sequence in the copolymers, MS/MS-ESI was applied on different selected polymer ions (Fig. S21†). However, the fragmentation spectra obtained showed different pathways for the same ion. In fact, the intensity values of the different peaks were affected

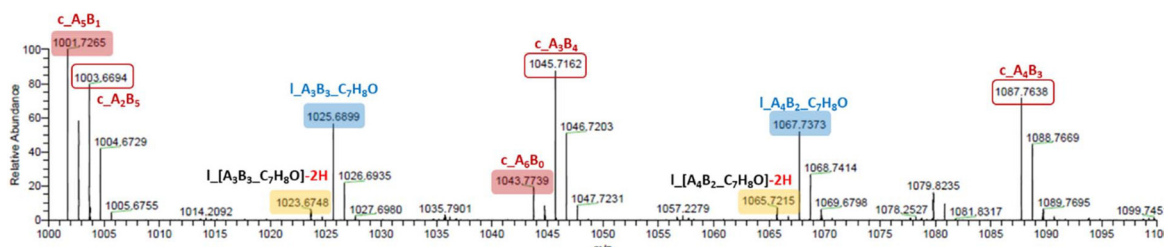


Fig. 5 Details ($m/z = 1000\text{--}1100$) of the high resolution ESI mass spectrum of a $\text{P}(\text{CL}^{\text{nBu}}\text{-co-CL}^{\text{Me}})$ copolymer prepared by the ROCOP of a 1:1 mixture of (*R*)- CL^{nBu} and (*S*)- CL^{Me} with the **1a**/BnOH catalytic system (Table 1, entry 3), showing resolved peaks for cyclic $\text{P}[(\text{CL}^{\text{nBu}})_5\text{-co-(CL}^{\text{Me}}\text{)}_5]$ (m/z_{exp} (all ^{12}C) = 1001.7265, $m/z_{\text{calcd}} = 1001.7263$), cyclic $\text{P}[(\text{CL}^{\text{nBu}})_2\text{-co-(CL}^{\text{Me}}\text{)}_5]$ (m/z_{exp} (all ^{12}C) = 1003.6694, $m/z_{\text{calcd}} = 1003.6692$), linear $\text{P}[(\text{CL}^{\text{nBu}})_3\text{-co-(CL}^{\text{Me}}\text{)}_3]\text{-C}_7\text{H}_8\text{O}$ – 2H (m/z_{exp} (all ^{12}C) = 1023.6748, $m/z_{\text{calcd}} = 1023.6743$), linear $\text{P}[(\text{CL}^{\text{nBu}})_3\text{-co-(CL}^{\text{Me}}\text{)}_3]\text{-C}_7\text{H}_8\text{O}$ (m/z_{exp} (all ^{12}C) = 1025.6899, $m/z_{\text{calcd}} = 1025.6900$), cyclic $\text{P}[(\text{CL}^{\text{nBu}})_6\text{-co-(CL}^{\text{Me}}\text{)}_0]$ (m/z_{exp} (all ^{12}C) = 1043.7739, $m/z_{\text{calcd}} = 1043.7733$), cyclic $\text{P}[(\text{CL}^{\text{nBu}})_3\text{-co-(CL}^{\text{Me}}\text{)}_4]$ (m/z_{exp} (all ^{12}C) = 1045.7162, $m/z_{\text{calcd}} = 1045.7162$), linear $\text{P}[(\text{CL}^{\text{nBu}})_4\text{-co-(CL}^{\text{Me}}\text{)}_2]\text{-C}_7\text{H}_8\text{O}$ – 2H (m/z_{exp} (all ^{12}C) = 1065.7215, $m/z_{\text{calcd}} = 1065.7213$), linear $\text{P}[(\text{CL}^{\text{nBu}})_4\text{-co-(CL}^{\text{Me}}\text{)}_2]\text{-C}_7\text{H}_8\text{O}$ (m/z_{exp} (all ^{12}C) = 1067.7369, $m/z_{\text{calcd}} = 1067.7369$), cyclic $\text{P}[(\text{CL}^{\text{nBu}})_4\text{-co-(CL}^{\text{Me}}\text{)}_3]$ (m/z_{exp} (all ^{12}C) = 1087.7638, $m/z_{\text{calcd}} = 1087.7631$); the population at $m/z = 1079.8325$ could not be identified.



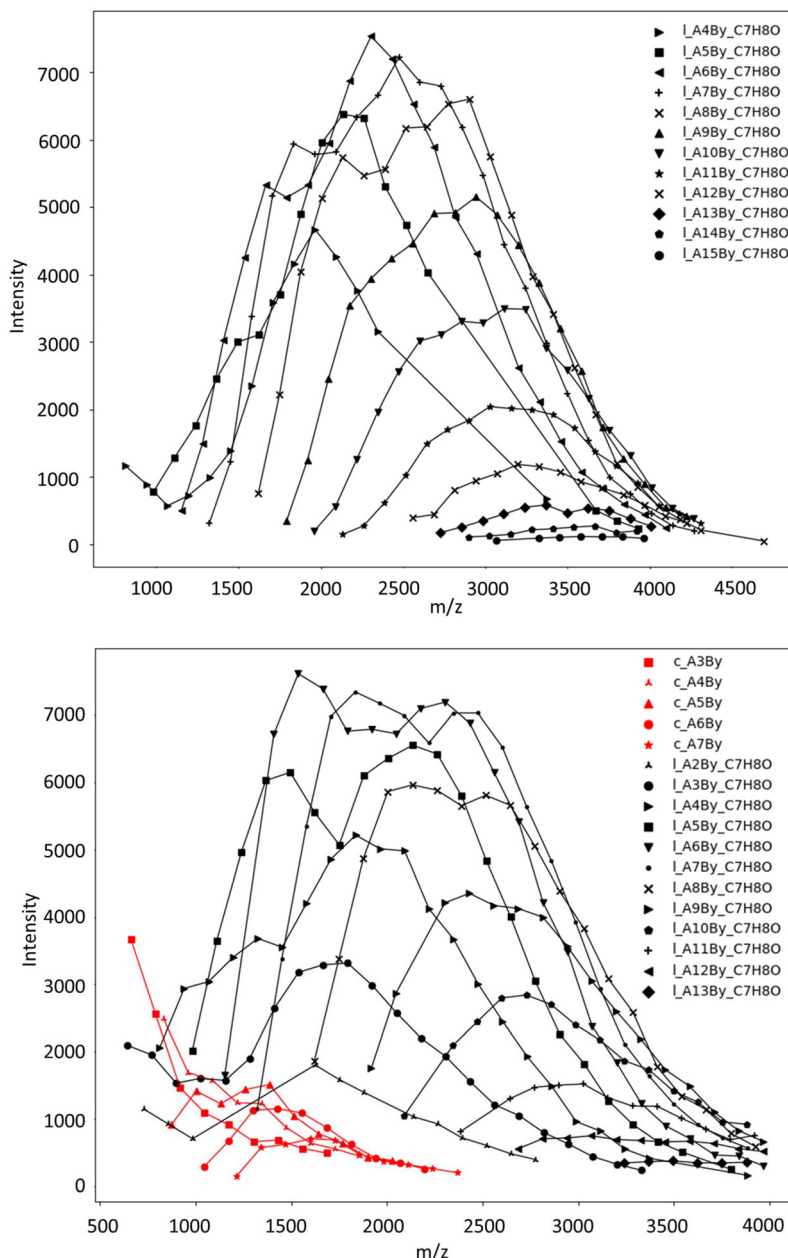


Fig. 6 Distribution of individual polymer series experimentally observed in MALDI-ToF mass spectra (DCTB matrix, ionized by Na^+ , data from Fig. 4) of $\text{P}(\text{CL}^{n\text{Bu}}\text{-co-CL}^{\text{Me}})$ copolymers prepared by the ROCOP of a 1:1 mixture of (R)- $\text{CL}^{n\text{Bu}}$ and (S)- CL^{Me} with the **1a**/BnOH catalytic system, over (a) 35 min and (b) 390 min, respectively (Table 1, entries 1 and 3, respectively) for m/z up to 4000. One or two major series of macromolecules, i.e. linear $\alpha\text{-BrO}_\omega\text{-OH-P}[(\text{CL}^{n\text{Bu}})_x\text{-co-(CL}^{\text{Me}})_y]$ (black series) and cyclic $\text{P}[(\text{CL}^{n\text{Bu}})_x\text{-co-(CL}^{\text{Me}})_y]$ (red series) populations, are distinguished. A_xB_y stands for x repeating units of A ($\text{CL}^{n\text{Bu}}$) and y repeating units of B (CL^{Me}).

by the overlap of signals within a narrow range, which makes this approach biased and eventually uninformative.

For this reason, the raw ESI and MALDI-ToF mass data were processed through a programmatic script *Polymers* (see the Experimental section). This enabled, for a given degree of polymerization (DP of $\text{P}[(\text{CL}^{n\text{Bu}})_x\text{-co-(CL}^{\text{Me}})_y] = x + y = \text{constant}$), the identification of all possible ionized macromolecular chains with different values of x and y ; these different possibilities were then adjusted in histograms displaying their relative intensities as a function of x . As illustrated in Fig. 7, the experi-

mental data for both the linear (blue) and cyclic (red) macromolecule populations, as determined from the ESI and MALDI-TOF mass data, follow the same trend. They also match quite well the whole distribution for a random copolymer (plotted in green), computed following a binomial distribution law. Essentially the same trend was observed for different DPs up to 26. In other words, the ROCOP of equimolar mixtures of (R)- $\text{CL}^{n\text{Bu}}$ and (S)- CL^{Me} with the **1a**/BnOH catalytic system leads to random-type copolymers; in case a highly alternating microstructure of the type $\text{P}[(\text{CL}^{n\text{Bu}}\text{-CL}^{\text{Me}})_n]$

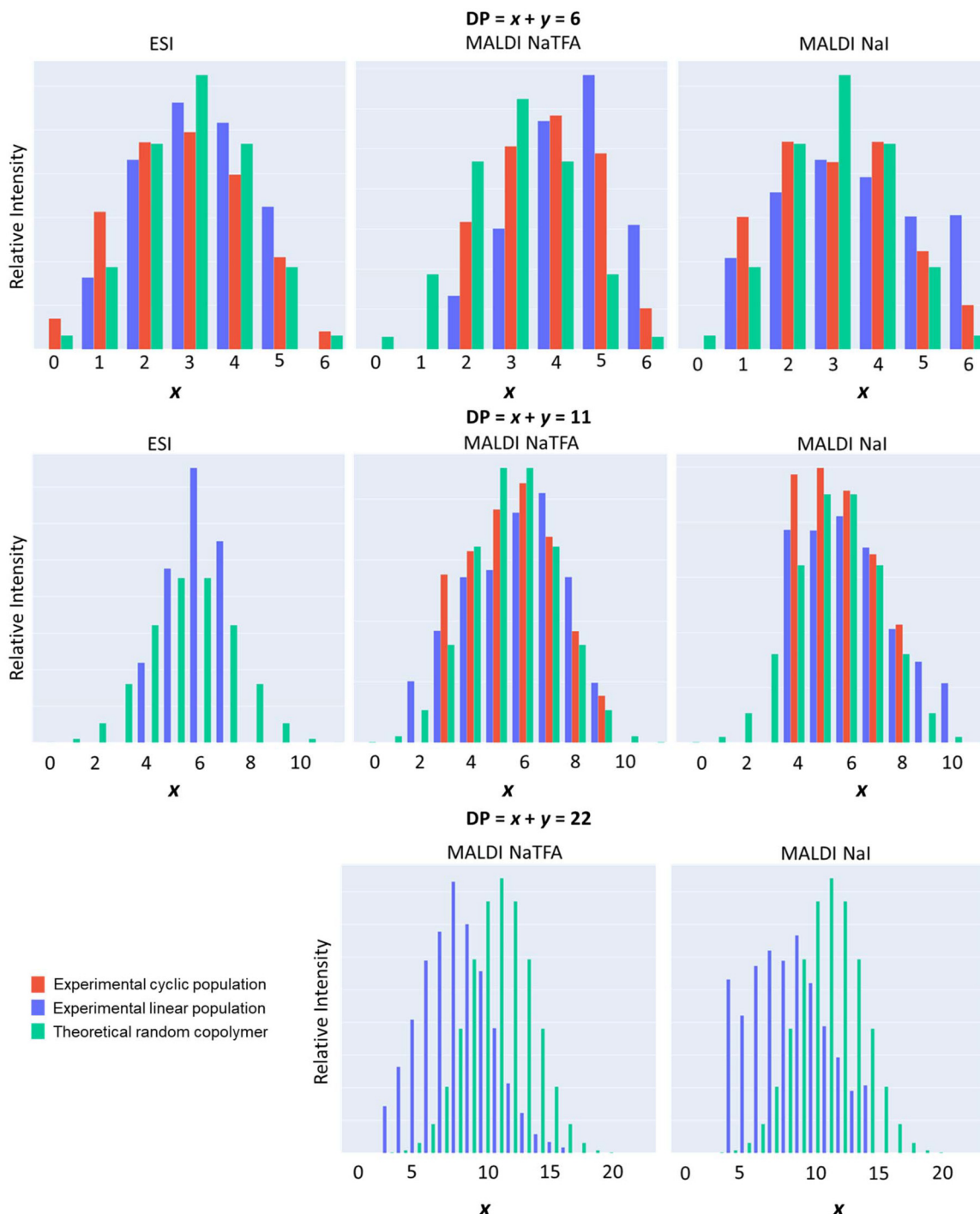


Fig. 7 Histograms of experimental (blue: linear and red: cyclic) macromolecular ion distributions in a $\text{P}[(\text{CL}^{n\text{Bu}})_x\text{-co-(CL}^{\text{Me}})_y]$ copolymer (Table 1, entry 3) for selected $\text{DP} = x + y = 6, 11$, and 22 extracted from (left) ESI HRMS, (middle) MALDI-ToF MS using $\text{CF}_3\text{CO}_2^- \text{Na}^+$, and (right) MALDI-ToF MS using $\text{Na}^+ \text{I}^-$ as an ionizing source, and compared to theoretical (green) random copolymer distribution calculated from a binomial law.

had formed, the above experimental histograms would have been narrowly centered on the $x \pm 1$ values.

Fig. 7 also reveals interesting patterns in how the $\text{CL}^{n\text{Bu}}$ and CL^{Me} comonomers are arranged within the chains. Short chains (e.g. $\text{DP} = 6$) have a slightly higher proportion of $\text{CL}^{n\text{Bu}}$ units compared to what is predicted theoretically. The distri-

bution of the comonomers in medium-length chains (e.g. $\text{DP} = 11$) is closer to what is expected based on a binomial distribution for a random copolymer. Conversely, long chains (e.g. $\text{DP} = 26$) have a lower proportion of $\text{CL}^{n\text{Bu}}$ units. Fig. 8 further exemplifies this trend by tracking the composition of the most intense monoisotopic m/z signal at different lengths (DPs). For



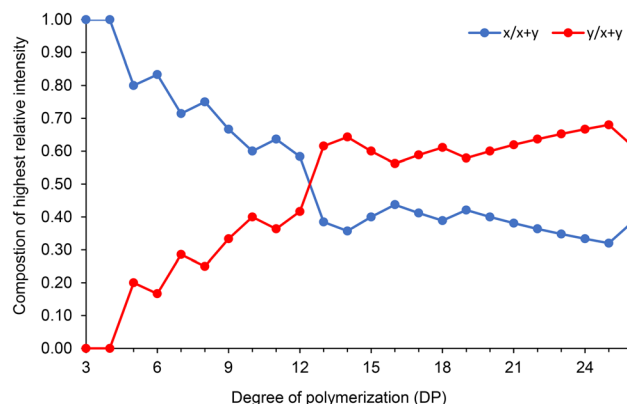


Fig. 8 Variation of the composition (x , y) in $P(CL^{nBu})_x\text{-co-}(CL^{Me})_y$ copolymers as a function of the degree of polymerization (DP). The composition was calculated from the most intense m/z signal for a defined DP, from MALDI-ToF MS of $P(CL^{nBu}\text{-co-}CL^{Me})$ copolymers prepared by the ROCOP of a 1:1 mixture of (R)- CL^{nBu} and (S)- CL^{Me} with the **1a**/BnOH catalytic system, over 35 min (Table 1, entry 1).

chains with $x + y = 13$ units, the amounts of CL^{nBu} and CL^{Me} are roughly equal. For shorter chains ($DP < 13$), there is a higher proportion of CL^{nBu} , while there is a higher content of CL^{Me} for longer chains ($DP > 13$). These uneven distributions point to gradient-type macromolecules which are likely formed through preferential polymerization of the more reactive CL^{Me} at early stages of the copolymerization reaction.

Böcker *et al.* developed a related method to determine similar parameters from a single MALDI-ToF MS analysis.²⁷ Their software (COCONUT) plots the matrix of mass data in a 3D graph where the x - and y -axes show the amount of each monomer in the copolymer, with the peak intensity displayed on the z -axis. The shape of the thus obtained counter-plots reflects the microstructure of the copolymer: when the contour plot is centered on a diagonal straight line that crosses the origin, with a narrow distribution along this line, then an alternating copolymer is formed (the narrower the contour plot, the higher the alternation degree); however, if the distri-

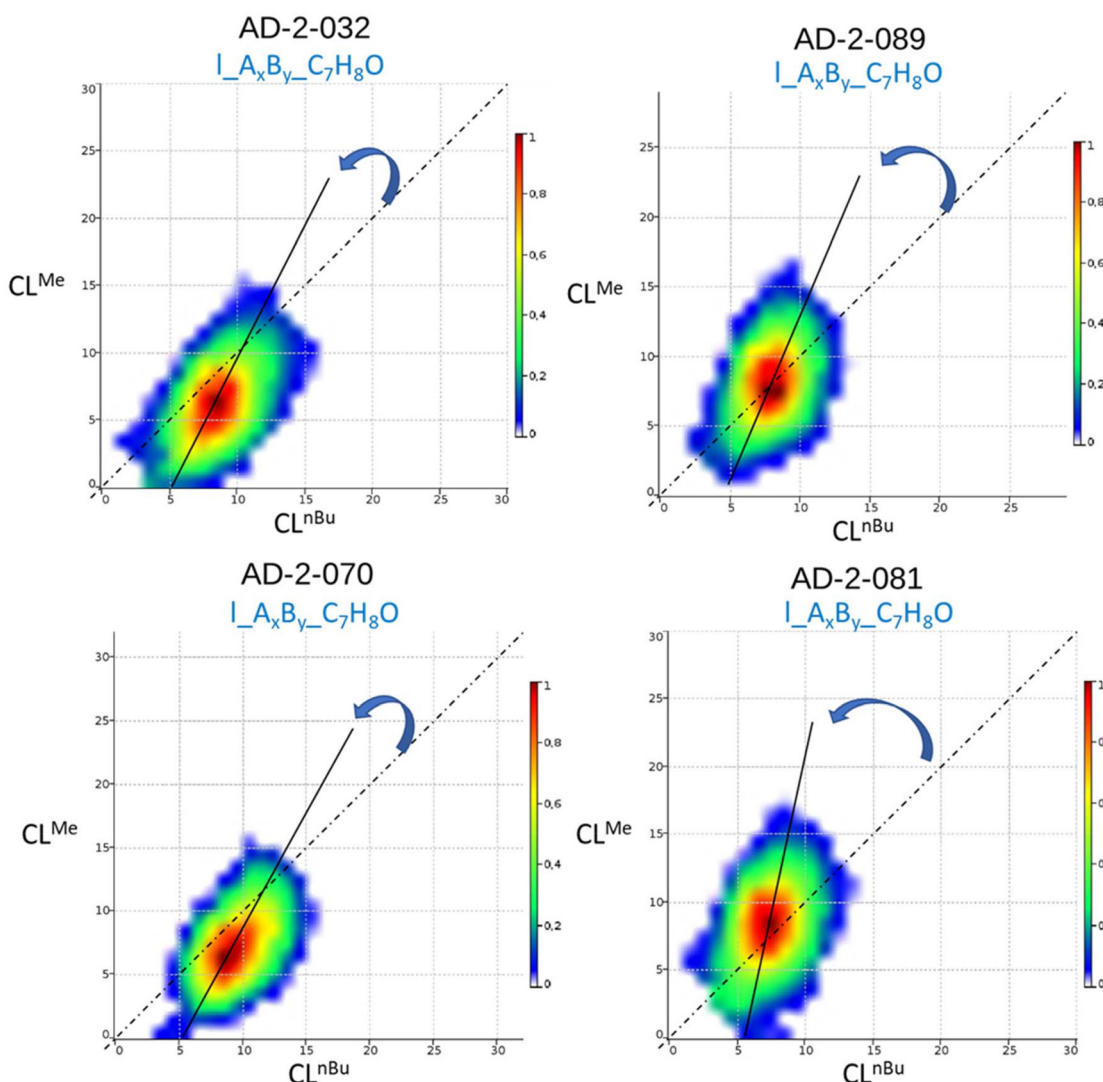


Fig. 9 Examples of contour-plots generated using the COCONUT software²⁴ from MALDI-ToF MS data of a $P(CL^{nBu})_x\text{-co-}(CL^{Me})_y$ copolymer (Table 1, left: entry 3, right: entry 1).

bution is broad, and passes through the origin, a random copolymer is obtained; on the other hand, if the contour plot deviates from the diagonal line, not going through the origin, then a gradient (composition drift) or a blocky structure is proposed.²⁵ The COCONUT software allows also the determination of the reactivity ratios from monomer distribution contour-plots. We analyzed the MALDI-ToF MS data of our $P(CL^{nBu})_x\text{-}co\text{-}(CL^{Me})_y$ copolymers using COCONUT, and examples of the resulting contour-plots are shown in Fig. 9. In all cases, the line drawn through the center of the broadly dispersed contour-plots is consistent with a gradient (*i.e.*, random with a composition drift) structure, with no alternation. The offset of the contour plots toward the y -axis indicates the higher reactivity of CL^{Me} compared to that of CL^{nBu} . The COCONUT software also allowed calculating from the copolymer distribution the reactivity ratios of both co-monomers ($r_{CL}^{nBu} = 0.10$ and $r_{CL}^{Me} = 1.94$), which is in line with a random gradient structure and the aforementioned observations.

In order to correlate the reactivity ratios of the two monomers derived from MS analysis, further experiments based on the Fineman–Ross method were performed (refer to the Experimental section, Fig. S12†). The thus calculated reactivity ratios ($r_{CL}^{nBu} = 0.19$ and $r_{CL}^{Me} = 1.02$) are consistent with the above values determined from the MS data with COCONUT. They point out at the formation of random copolymers (with a composition drift), which eventually reflects the lack of stereocontrol of the yttrium achiral catalyst over seven-membered substituted- ϵ -caprolactones.

Conclusion

Yttrium complexes based on tetradentate non-chiral diamino-bis(*o,p*-disubstituted-phenolate) ligands effectively (co)polymerize 1-substituted- ϵ -caprolactones such as CL^{Me} and CL^{nBu} . 1H and ^{13}C NMR spectroscopy confirmed the general structure of the (co)polymers formed and the good control over the molar masses, as also supported by SEC analyses. However, the NMR spectroscopic method remained insufficient for analyzing the (co)polymers' microstructures and, in particular, for assessing the tacticity of the homopolymers. The ROCOP of equimolar mixtures of enantiopure comonomers with opposite configurations, (*R*)- CL^{nBu} and (*S*)- CL^{Me} , returned copolymers whose microstructure/comonomer sequence could be only, but effectively, deciphered by detailed MS analyses. The latter studies provided solid evidence for the formation of gradient copolymers. The non-alternating monomer sequence in these copolymers evidences that the yttrium catalysts used failed to differentiate between the two opposite-configuration monomers. In turn, this lack of alternation during copolymerization evidences the absence of significant syndioselectivity of these yttrium catalysts in the homopolymerization of *rac*- CL^{Me} and *rac*- CL^{nBu} . This contrasts drastically with the good stereoselectivities towards syndiotactic, or even isotactic, polyesters that these $Y\{ON(N)O^{R2}\}$ catalysts have shown in the ROP of a variety of racemic β -lactones, lactides and diolides. These obser-

vations made for the two catalysts and two monomers selected in the present study allow conclusions which, of course, should be extrapolated only with caution (as for all extrapolation in science). Despite the limited stereoelectronic difference in the R substituents (*i.e.*, Me vs. *n*Bu) of the two CL^R monomers (corroborated by the small difference in their ROP reaction rates), a different outcome may be observed with even less differentiated monomers (*e.g.* R = Me vs. Et) or, obviously, different catalytic systems with better stereocontrol ability.

Author contributions

Ali Dhaini: investigation, formal analysis, writing – original draft, review and editing. Jérôme Ollivier: mass spectrometry analysis, formal analysis, data curation, writing – original draft, review and editing. Nicolas Le Yondre: mass spectrometry analysis, MS software, and writing – original draft. Ali Alaeddine: supervision. Sophie M Guillaume: writing – original draft, review & editing, supervision, formal analysis, and conceptualization. Jean-François Carpentier: writing – original draft, review and editing, supervision, formal analysis, and conceptualization.

Data availability

The raw data required to reproduce these findings are available from the authors. The processed data required to reproduce these findings are available in the ESI.†

Conflicts of interest

The authors declare no conflicts of interest.

Acknowledgements

This research was financially supported in part by the University of Rennes (Ph.D. grant to A. D.) and the Lebanese University (Ph.D. grant to A. D.). We are grateful to CRMPO and UAR ScanMAT (CNRS, Univ. Rennes), especially to Philippe Jéhan and Elsa Caytan, for MS and NMR analyses, respectively. We thank Maxime Lanvin for the development of the MS data-processing script. We thank Dr Martin Engler-Lukajewski (Bright Giant GmbH) for useful discussions regarding the exploitation of the COCONUT software.

References

- For recent leading reviews on metal-catalyzed ROP of lactones and related derivatives, see: (a) S. M. Guillaume, E. Kirillov, Y. Sarazin and J.-F. Carpentier, *Beyond stereoselectivity, switchable catalysis: some of the last frontier challenges in ring-opening polymerization of cyclic esters*,



Chem. – Eur. J., 2015, **21**, 7988–8003; (b) X. Tang and E. Y.-X. Chen, Toward infinitely recyclable plastics derived from renewable cyclic esters, *Chem.*, 2019, **5**, 284–312; (c) J. C. Worch, H. Prydderch, S. Jimaja, P. Bexis, M. L. Becker and A. P. Dove, Stereochemical enhancement of polymer properties, *Nat. Rev. Chem.*, 2019, **3**, 514–535; (d) M. J.-L. Tschan, R. M. Gauvin and C. M. Thomas, Controlling polymer stereochemistry in ring-opening polymerization: a decade of advances shaping the future of biodegradable polyesters, *Chem. Soc. Rev.*, 2021, **50**, 13587–13608; (e) C. M. Plummer, L. Li and Y. Chen, Ring-opening polymerization for the goal of chemically recyclable polymers, *Macromolecules*, 2023, **56**, 731–750; (f) X. Xie, Z. Huo, E. Jang and R. Tong, Recent advances in enantioselective ring-opening polymerization and copolymerization, *Nat. Commun. Chem.*, 2023, **6**, 202; (g) L. Al-Shok, D. M. Haddleton and F. Adams, Progress in catalytic ring-opening polymerization of biobased lactones, in *Synthetic biodegradable and biobased polymers: Industrial aspects and technical products*, ed. A. Kunkel, G. Battagliarin, M. Winnacker, B. Rieger and G. Coates, Springer Internat. Pub, Cham, 2024, pp. 197–267.

2 J.-F. Carpentier, Rare-earth complexes supported by tripodal tetradentate bis(phenolate) ligands: A privileged class of catalysts for ring-opening polymerization of cyclic esters, *Organometallics*, 2015, **34**, 4175–4189.

3 (a) A. Amgoune, C. M. Thomas and J.-F. Carpentier, Controlled ring-opening polymerization of lactide by group 3 metal complexes, *Pure Appl. Chem.*, 2007, **79**, 2013–2030; (b) C. X. Cai, A. Amgoune, C. W. Lehmann and J.-F. Carpentier, Stereoselective ring-opening polymerization of racemic lactide using alkoxy-amino-bis(phenolate) group 3 metal complexes, *Chem. Commun.*, 2004, 330–331; (c) A. Amgoune, C. M. Thomas, T. Roisnel and J.-F. Carpentier, Ring-opening polymerization of lactide with group 3 metal complexes supported by dianionic alkoxy-amino-bisphenolate ligands: Combining high activity, productivity, and selectivity, *Chem. – Eur. J.*, 2005, **12**, 169–179; (d) A. Amgoune, C. M. Thomas and J.-F. Carpentier, Yttrium complexes as catalysts for living and immortal polymerization of lactide to highly heterotactic PLA, *Macromol. Rapid Commun.*, 2007, **28**, 693–697.

4 (a) N. Ajellal, M. Bouyahyi, A. Amgoune, C. M. Thomas, A. Bondon, I. Pillin, Y. Grohens and J.-F. Carpentier, Syndiotactic-enriched poly(3-hydroxybutyrate)s via stereoselective ring-opening polymerization of racemic β -butyrolactone with discrete yttrium catalysts, *Macromolecules*, 2009, **42**, 987–993; (b) A. Amgoune, C. M. Thomas, S. Ilinca, T. Roisnel and J.-F. Carpentier, Highly active, productive, and syndiospecific yttrium initiators for the polymerization of racemic β -butyrolactone, *Angew. Chem., Int. Ed.*, 2006, **45**, 2782–2784.

5 For recent examples of other highly efficient yttrium catalysts for stereoselective ROP of *rac*-BPL^{Me}, see: (a) H.-Y. Huang, W. Xiong, Y.-T. Huang, K. Li, Z. Cai and

J.-B. Zhu, Spiro-Salen catalysts enable the chemical synthesis of stereoregular polyhydroxylalkanoates, *Nat. Catal.*, 2023, **6**, 720–728; (b) J. Bruckmoser, S. Pongratz, L. Stieglitz and B. Rieger, Highly isoselective ring-opening polymerization of *rac*- β -butyrolactone: Access to synthetic poly(3-hydroxybutyrate) with polyolefin-like material properties, *J. Am. Chem. Soc.*, 2023, **145**, 11494–11498.

6 R. Ligny, M. M. Hanninen, S. M. Guillaume and J.-F. Carpentier, Highly syndiotactic or isotactic polyhydroxylalkanoates by ligand-controlled yttrium-catalyzed stereoselective ring-opening polymerization of functional racemic β -lactones, *Angew. Chem., Int. Ed.*, 2017, **56**, 10388–10393.

7 (a) R. M. Shakaroun, A. Dhaini, R. Ligny, A. Alaaeddine, S. M. Guillaume and J.-F. Carpentier, Stereo-electronic contributions in yttrium-mediated stereoselective ring-opening polymerization of functional racemic β -lactones: ROP of 4-alkoxymethylene- β -propiolactones with bulky exocyclic chains, *Polym. Chem.*, 2023, **14**, 720–727; (b) R. M. Shakaroun, H. Li, P. Jéhan, M. Blot, A. Alaaeddine, J.-F. Carpentier and S. M. Guillaume, Stereoselective ring-opening polymerization of functional β -lactones: influence of the exocyclic side-group, *Polym. Chem.*, 2021, **12**, 4022–4034.

8 J. W. Kramer, D. S. Treitler, E. W. Dunn, P. M. Castro, T. Roisnel, C. M. Thomas and G. W. Coates, Polymerization of enantiopure monomers using syndiospecific catalysts: A new approach to sequence control in polymer synthesis, *J. Am. Chem. Soc.*, 2009, **131**, 16042–16044.

9 C. G. Jaffredo, Y. Chapurina, S. M. Guillaume and J.-F. Carpentier, From syndiotactic homopolymers to chemically tunable alternating copolymers: Highly active yttrium complexes for stereoselective ring-opening polymerization of β -malolactonates, *Angew. Chem., Int. Ed.*, 2014, **53**, 2687–2691.

10 (a) X. Tang and E. Y.-X. Chen, Chemical synthesis of perfectly isotactic and high melting bacterial poly(3-hydroxybutyrate) from bio-sourced racemic cyclic diolide, *Nat. Commun.*, 2018, **9**, 2345–2356; (b) E. Y.-X. Chen and X. Tang, Synthesis of crystalline polymers from cyclic diolides, *US Pat. Appl.*, 2019, 0211144; (c) X. Tang, A. H. Westlie, E. M. Watson and E. Y.-X. Chen, Stereosequenced crystalline polyhydroxylalkanoates from diastereomeric monomer mixtures, *Science*, 2019, **366**, 754–758; (d) Z. Zhang, C. Shi, M. Scoti, X. Tang and E. Y.-X. Chen, Alternating isotactic polyhydroxylalkanoates via site- and stereoselective polymerization of unsymmetrical diolides, *J. Am. Chem. Soc.*, 2022, **144**, 20016–20024; (e) E. C. Quinn, A. H. Westlie, A. Sangroniz, M. R. Caputo, S. Xu, Z. Zhang, M. Urgun-Demirtas, A. J. Muller and E. Y.-X. Chen, Installing controlled stereo-defects yields semicrystalline and biodegradable poly(3-hydroxybutyrate) with high toughness and optical clarity, *J. Am. Chem. Soc.*, 2023, **145**, 5795–5802.

11 (a) E. Archer, M. Torretti and S. Madbouly, Biodegradable polycaprolactone (PCL) based polymer and composites, *Phys. Sci. Rev.*, 2023, **8**, 4391–4414; (b) M. Labet and



W. Thielemans, Synthesis of polycaprolactone: a review, *Chem. Soc. Rev.*, 2009, **38**, 3484–3504; (c) M. A. Woodruff and D. W. Hutmacher, The return of a forgotten polymer. Polycaprolactone in the 21st century, *Prog. Polym. Sci.*, 2010, **35**, 1217–1256; (d) A. L. Sisson, D. Ekinci and A. Lendlein, The contemporary role of ϵ -caprolactone chemistry to create advanced polymer architectures, *Polymer*, 2013, **54**, 4333–4350.

12 F. J. van Natta, J. W. Hill and W. H. Carothers, Studies of Polymerization and Ring Formation. XXIII.¹ ϵ -Caprolactone and its Polymers, *J. Am. Chem. Soc.*, 1934, **56**, 455–457.

13 (a) *Encyclopedia of polymer science and engineering*, ed. F. F. Mark, N. Bikales, C. Overberger, G. Menges and J. Kroshwitz, John Wiley and Sons, New York, 1985, pp. 220–243; (b) M. Okada, Chemical syntheses of biodegradable polymers, *Prog. Polym. Sci.*, 2002, **27**, 87–133; (c) L. S. Nair and C. T. Laurencin, Biodegradable polymers as biomaterials, *Prog. Polym. Sci.*, 2007, **32**, 762–798.

14 (a) A. Watts, N. Kurkokawa and M. A. Hillmyer, Efficient polymerization of methyl- ϵ -caprolactone mixtures to access sustainable aliphatic polyesters, *Biomacromolecules*, 2017, **18**, 1845–1854; (b) D. C. Batiste, M. S. Meyersohn, A. Watts and M. A. Hillmyer, Efficient polymerization of methyl- ϵ -caprolactone mixtures to access sustainable aliphatic polyesters, *Macromolecules*, 2020, **53**, 1795–1808; (c) G. X. De Hoe, M. T. Zumstein, B. J. Tiegs, J. P. Brutman, K. McNeill, M. Sander, G. W. Coates and M. A. Hillmyer, Sustainable polyester elastomers from lactones: Synthesis, properties, and enzymatic hydrolyzability, *J. Am. Chem. Soc.*, 2018, **140**, 963–973.

15 P. Vangeye and R. Jérôme, Amphiphilic block copolymers of high-molecular-weight poly(ethylene oxide) and either ϵ -caprolactone or γ -methyl- ϵ -caprolactone: Synthesis and characterization, *J. Polym. Sci., Part A*, 2004, **42**, 1132–1142.

16 C. Wang, Y. Xiao, A. Heise and M. Lang, Organometallic and enzymatic catalysis for ring opening copolymerization of ϵ -caprolactone and 4-methyl- ϵ -caprolactone, *J. Polym. Sci., Part A*, 2011, **49**, 5293–5300.

17 Y.-M. Tu, F.-L. Gong, Y.-C. Wu, Z. Cai and J.-B. Zhu, Insights into substitution strategy towards thermodynamic and property regulation of chemically recyclable polymers, *Nat. Commun.*, 2023, **14**, 3198.

18 J. Kiriratnikom, C. Robert, V. Guerineau, V. Vendtiiito and C. M. Thomas, Stereoselective ring-opening (co)polymerization of β -butyrolactone and ϵ -decalactone using an yttrium bis(phenolate) catalytic system, *Front. Chem.*, 2019, **7**, 301.

19 C. Lv, G. Xu, R. Yang, L. Zhou and Q. Wang, Stereogradient polycaprolactones formed by asymmetric kinetic resolution polymerization of 6-methyl- ϵ -caprolactone, *Polym. Chem.*, 2021, **12**, 4856–4863.

20 M. Bouyahyi, N. Ajellal, E. Kirillov, C. M. Thomas and J.-F. Carpentier, Exploring electronic versus steric effects in stereoselective ring-opening polymerization of lactide and β -butyrolactone with amino-alkoxy-bis(phenolate)-yttrium complexes, *Chem. – Eur. J.*, 2011, **17**, 1872–1883.

21 M. Fineman and S. D. Ross, Linear method for determining monomer reactivity ratios in copolymerization, *J. Polym. Sci.*, 1950, **5**, 259–265.

22 (a) L. R. Rieth, D. R. Moore, E. B. Lobkovsky and G. W. Coates, Single-site β -diimine zinc catalysts for the ring-opening polymerization of β -butyrolactone and β -valerolactone to poly(3-hydroxyalkanoates), *J. Am. Chem. Soc.*, 2002, **124**, 15239–15248; (b) B. M. Chamberlain, M. Cheng, D. R. Moore, T. M. Ovitt, E. B. Lobkovsky and G. W. Coates, *J. Am. Chem. Soc.*, 2001, **123**, 3229–3238.

23 DSC analyses of the prepared homo- and copolymers revealed no distinctive thermal properties (see Tables S1 and 1†): all polymers are essentially amorphous (no melting transition observed under our analytical conditions; Table S1†) and all have glass transition temperatures in the same range.

24 As mentioned previously, the nearly perfect alternating copolymers obtained from 1 : 1 mixtures of (S)-MLA^{Bn} and (R)-MLA^{All} using Y{ON(X)O^{R2}} catalysts evidence limited stereoelectronic difference in the R substituents (*i.e.*, benzyl vs. allyl).⁸ Also, using the same catalytic system, the ROCOP of 1 : 1 mixtures of (R)-BPL^{OMe} and (S)-BPLOTBDMS (OTBDMS = OSi₂BU₂Me₂) returned a copolymer with up to 67% alternation, despite the more pronounced steric difference between OMe and OTBDMS. Decreasing the stereoelectronic difference between R groups, as with mixtures of BPL^{OBn} and BPL^{OMe}, increased the degree of alternation to 89% (see: R. Ligny, S. M. Guillaume and J.-F. Carpentier, Yttrium-mediated ring-opening copolymerization of oppositely configurated 4-alkoxymethylene- β -propiolactones: Effective access to highly alternated isotactic functional PHAs, *Chem. Eur. J.*, 2019, **25**, 6412–6424). Coates, *et al.* also reported the formation of highly alternating copolymers using yttrium salan complexes by the ROCOP of 1 : 1 mixtures of enantiopure, opposite-configuration BPLRs (R = Me and R = *t*Bu), overcoming kinetic considerations where the reaction is under stereocontrol.⁷

25 (a) S. Huijser, B. B. Staal, J. Huang, R. Duchateau and C. E. Koning, Chemical composition and topology of poly(lactide-*co*-glycolide) revealed by pushing MALDI-ToF MS to its limit, *Angew. Chem., Int. Ed.*, 2006, **45**, 4104–4108; (b) S. Huijser, G. D. Mooiweer, R. van der Hofstad, B. B. Staal, J. Feenstra, A. M. van Herk, C. E. Koning and R. Duchateau, Reactivity ratios of comonomers from a single MALDI-ToF-MS measurement at one feed composition, *Macromolecules*, 2012, **45**, 4500–4510.

26 R. X. Willemse, B. B. Staal, E. H. Donkers and A. M. van Herk, Copolymer fingerprints of polystyrene-*block*-polyisoprene by MALDI-ToF-MS, *Macromolecules*, 2004, **37**, 5717–5723.

27 M. S. Engler, S. Crotty, M. J. Barthel, C. Pietsch, K. Knop, U. S. Schubert and S. Böcker, COCONUT-An efficient tool for estimating copolymer compositions from mass spectra, *Anal. Chem.*, 2015, **87**, 5223–5231.

28 J. Stouten, M. A. F. Delgove, N. De Vos, K. Matthysen, G. G. P. Deroover and K. V. Bernaerts, Investigation of monomer reactivity, polymer microstructure and solubility in the copolymerization of 1,5-dioxepan-2-one with alkyl substituted lactones, *Eur. Polym. J.*, 2023, **200**, 112523.



29 B. Staal, *Characterization of (co)polymers by MALDI-TOF-MS*, Ph.D. Thesis, University of Technology Eindhoven, The Netherlands, 2005.

30 O. Trhlíková, M. Janata, Z. Walterová, L. Kanizsová, E. Čadová and J. Horský, MALDI-ToF mass spectrometry detection of intramolecular composition gradient in copolymers, *Talanta*, 2019, **195**, 215–220.

31 Besides the linear α -BnO, ω -OH-[P(CL^{nBu})_x-co-(CL)_y] and the cyclic [P(CL^{nBu})_x-co-(CL^{Me})_y] major series, another minor

population was also observed in the ESI mass spectra – at e.g. m/z = 981.6271, 1023.6748, 1065.7215, that apparently corresponds to linear α -BnO, ω -OH-[P(CL^{nBu})_x-co-(CL)_y] macromolecules deprived of two hydrogens (see Fig. 5 and S14, S16, S18†). We assume that this population formed during the ESI MS ionization process (presumably by the loss of hydrogen atoms to form α,β -unsaturated ester within the main chain); no unsaturated groups were detected in the NMR spectra of the crude and reprecipitated copolymers.

